Chapter 5 Biosynthesis of Metallic Nanoparticles and their Applications

Capítulo 5 Biosíntesis de Nanopartículas Metálicas y sus Aplicaciones

REYES-PÉREZ, Jazmin A.[1]†, ROA-MORALES, Gabriela[1]*, AMAYA-CHÁVEZ, Araceli[2] and BALDERAS-HERNÁNDEZ, Patricia[1]

[1]Universidad Autónoma del Estado de México, (UAEMex), Centro Conjunto de Investigación en Química Sustentable (CCIQS) UAEM-UNAM, Carretera Toluca-Atlacomulco, Km 14.5, Toluca, MEX, México. 50200.
[2]Universidad Autónoma del Estado de México, Faculty of Chemistry, Paseo Colón, Colonia Universidad, Toluca de Lerdo, MEX, México. 50120

ID 1st Author: *Jazmin A., Reyes-Pérez* / **ORC ID:** 0000-0002-5341-1829, **CVU CONACYT ID**: 700495

ID 1st Co-author: *Gabriela, Roa-Morales* / **ORC ID:** 0000-0001-7355-2568, **CVU CONACYT ID**: 121592

ID 2nd Co-author: *Araceli, Amaya-Chávez* / **ORC ID:** 0000-0001-9798-0882, **CVU CONACYT ID**: 201356

ID 3rd Co-author: *Patricia, Balderas-Hernández* / **ORC ID:** 0000-0001-6214-6599, **CVU CONACYT ID**: 120896

DOI: 10.35429/H.2021.3.87.121

A. Marroquín, J. Olivares, D. Ventura and L. Cruz (Coord) Agricultural Sciences and Biotechnology. Handbooks-©ECORFAN-México, Querétaro, 2021.

Abstract

The development of nano-sized materials increasingly requires the implementation of synthesis methods that are friendly to the environment and that have the ability to implement them in medical, therapeutic, pharmacological, food and environmental areas. As such, green methods have been gaining ground in recent years. Within these processes, there is a huge range of species belonging to different groups (such as bacteria, algae, yeasts, fungi, and plants) with the necessary qualities to generate metallic NPs with particular size and shape characteristics, within which plants stand out. This is due to the simplicity of the process as well as their easy scaling. Additionally, the studies carried out indicate the parameters to be considered in order to carry out a good bioreduction process and obtain both monometallic and highly functional bimetallic nanoparticles. It should be noted that in addition to the economic and ecological advantages of the nature of these methods, the biological molecules that participate as reducing agents also provide stability to the NPs, in some cases conferring superior qualities in catalytic and clinical applications.

Bioreduction, Vegetal extract, Phytochemicals, Catalyst

Resumen

El desarrollo de materiales nanométricos requiere cada vez más la implementación de métodos de síntesis amigables con el ambiente y que tengan la capacidad de implementarlos en los ámbitos médico, terapéutico, farmacológico, alimentario y medioambiental. Como tal, los métodos ecológicos han ido ganando terreno en los últimos años. Dentro de estos procesos, existe una amplia gama de especies pertenecientes a diferentes grupos (como bacterias, algas, levaduras, hongos y plantas) con las cualidades necesarias para generar NP metálicas con características particulares de tamaño y forma, dentro de las cuales destacan las plantas. Esto se debe a la simplicidad del proceso, así como a su fácil escalado. Además, los estudios realizados indican los parámetros a considerar para llevar a cabo un buen proceso de biorreducción y obtener nanopartículas tanto monometálicas como bimetálicas altamente funcionales. Cabe señalar que además de las ventajas económicas y ecológicas de la naturaleza de estos métodos, las moléculas biológicas que participan como agentes reductores también brindan estabilidad a las NP, en algunos casos confiriendo cualidades superiores en aplicaciones catalíticas y clínicas.

Biorreducción, Extracto vegetal, Fitoquímicos, Catalizador

1. Introduction

Nanotechnology is a fascinating multi-disciplined field that involves the design and engineering of functional systems on the molecular scale. It can be defined as the art and the science of the manipulation of matter at the nanoscale to create new and unique materials. Its main characteristic is a dimensional structure smaller than 100 nm, which is important in the fields of materials science, medical and life sciences, and physical and chemical sciences (Nayantara & Kaur, 2018; Vijayaraghavan & Ashokkumar, 2017). They mainly present themselves in characteristics such as catalytic reactivity, thermal conductivity, nonlinear optical behavior, and chemical stability, owing to their high surface-area-to-volume (Agarwal et al., 2017).

The development of metallic nanoparticles has been integrated in diverse areas such as medicine, chemistry, engineering, and biology, as well as participating in industries such as cosmetics, food, pharmaceuticals. It is equally involved in the development of new technologies for the detection, cleaning, and prevention of contamination. It is estimated that the global market of nanoparticles in biotechnology and pharmaceuticals grew by up to $79.8 billion in 2019, and that it will continue growing by around 22% annually (Nayantara & Kaur, 2018; Scaria et al., 2020). The synthesis and assembly of nanoparticles through biological routes allows the development of clean, non-toxic, and environmentally acceptable procedures involving organisms that vary from bacterias to bigger plants. The three main aspects of bioreduction related with the principles of green chemistry are: 1) the choice of non-toxic solvents for the reduction reaction, as distilled water is generally used in green synthesis. This is done to avoid the use of toxic organic solvents which are usual in chemical synthesis such as ethanol, dimethylformamide, ethylene glycol, toluene, and chloroform, owing to the use of hydrophobic stabilizing agents. 2) environmentally benign reducing agents and non-harmful stabilizing agents which form part of the biomolecules of the used organisms.

Many of these have the capacity to act as reducers and stabilizers in a simultaneous manner, substituting the use of chemical compounds such as sodium borohydride, hydrazine, and elemental hydrogen as reducing agents and the use of natural or synthetic polymers such as rubber, chitosan, cellulose, and copolymer micelles as stabilizers. In this sense the recovery that the biomolecules provide on the surface of the NPs makes them biocompatible, opening the possibility of applications in biomedicine and related fields (Gan & Li, 2012; Nayantara & Kaur, 2018; D. Sharma et al., 2019).

1.1 Basic Approaches

The synthesis methods for nanoparticles are commonly classified by two main categories: 1) from top to bottom or 'Top down'. 2) from bottom to top or 'Bottom up' (Carrillo-Inungaray et al., 2018).

The 'Top down' approach is based on mechanical size reduction methods, gradually breaking down the volume of the material into structures on the nanoscale, using lithographic techniques such as: grinding, milling, sputtering, and thermic or laser ablation (Agarwal et al., 2017; Chinnasamy et al., 2018; Gan & Li, 2012; Vijayaraghavan & Ashokkumar, 2017).

The 'Bottom up' approach is based on assembly through smaller entities in the nanoscale range (10-100 nm) such as atoms or molecules. Based mainly on chemical and biological methods, this approach increases the possibility of producing more chemically homogenous metallic particles with less defects (Agarwal et al., 2017; Chinnasamy et al., 2018; Gan & Li, 2012; Narayanan & Sakthivel, 2010b; Vijayaraghavan & Ashokkumar, 2017).

Nanoparticles have physical, chemical, electronic, electric, mechanical, magnetic, thermic, dielectric, optic and biological properties and characteristics. These are generated by the reduction of their dimension regarding their atomic surface, surface energy, the reduction of imperfections and spatial confinement, which are in summary size, shape, and crystalline structure (Anu et al., 2020; Narayanan & Sakthivel, 2010).

2. Methods to obtain nanoparticles

In accordance with the approach that is chosen for obtaining metallic nanoparticles, physical or chemical methods were used. As was previously mentioned, the 'Top down' approach is mostly related to physical methods, whilst the 'Bottom up' approach is mainly related to distinct chemical methods.

2.1 Physical methods

Physical methods include laser ablation, evaporation-condensation, ball milling, plasma arcs, and mechano-chemical synthesis, among others (Jamkhande et al., 2019).

Laser ablation

This is a technique that produces colloidal nanoparticles in a variety of solvents, taking place in a vacuum chamber in the presence of certain inert gases. The solid material sits under a thin layer and is exposed to irradiation with a pulsed laser, mainly the Nd: YAG laser (yttrium-aluminium-garnet doped with neodymium) to an output of 106 μm, and their Ti: Sapphire harmony laser (sapphire doped with titanium). The irradiation of material through lasers leads to the fragmentation of solid material in the shape of nanoparticles, which stay in the liquid that surrounds the target and produce a colloidal solution. The duration and energy of the pulse laser determine the relative quantity of atoms and particles that form. Parameters, such as the duration of the laser pulse, the wavelength, the ablation time, the laser fluidity, and the average effective surrounding liquid with or without surfactant, influence the efficiency of the ablation and the characteristics of the formed particles (Jamkhande et al., 2019; Vijayaraghavan & Ashokkumar, 2017).

It is a relatively simple and efficient technique for obtaining large quantities of nanometric particles in the form of a suspension. Their properties can change in accordance with the used laser and the nature of the suspension. Another important advantage is the absence of chemical reagents in the solutions (Jamkhande et al., 2019; Vijayaraghavan & Ashokkumar, 2017).

Evaporation-condensation

This is generally performed using a tubular oven at atmospheric pressure. The source or original material collects in a container centered in the oven which evaporates in a carrier gas. However, the synthesis of nanoparticles using a tube oven at atmospheric pressure has some disadvantages: for example, the tube oven occupies a large space, consumes a large amount of energy whilst elevating the environmental temperature around the original material and requires a lot of time to achieve thermal stability (Vijayaraghavan & Ashokkumar, 2017).

High-energy ball milling

This is a mechanical technique that can be affected by certain variables in the process. It is classified between low energy and high energy milling, depending on the induced mechanical energy to the powder mix. The nanometric particles are produced through a process of high-energy ball milling, and this method is mainly used for the synthesis of intermetallic nanoparticles. The procedure consists of placing a large amount of the powder of the material you wish to reduce into a container together with various heavy balls. A high mechanical energy is applied to the powdered material with the help of a high-speed rotating ball (Jamkhande et al., 2019). The reduction of the particle size can be carried out using different high energy mills: those with attrition balls, planetary balls, vibrating balls, and low energy rotation. In each of these methods, the high energy heavy balls move freely, and can roll above the surface of the chamber that contains the ground material in a series of parallel layers. Alternatively, they can also fall freely and impact the powder. These high impact collisions reduce the material without generating chemical changes (Jamkhande et al., 2019; Vijayaraghavan & Ashokkumar, 2017).

Plasma arc technique

The high temperatures associated with the formation of the arc or plasma are used to effectively separate the atomic species of the prime matter. These are quickly recombined outside of the plasma to form nanometric sized particles (Vijayaraghavan & Ashokkumar, 2017).

2.2 Chemical methods

Chemical methods include chemical reduction, microemulsion, thermal decomposition, sol-gel, solvothermal, and electrochemical deposition.

Chemical reduction

Ionic salt is reduced in an appropriate way in the presence of a surfactant using different reducing agents. The formed metal nanoparticles are stabilized using trisodium citrate (TSC) or sodium lauryl sulfate (SLS). On occasion a stabilizing agent is used together with a reducing agent. The most common reducing agents are Sodium borohydride ($NaBH_4$), Potassium bitartrate ($KC_4H_5O_6$), glucose, ethylene glycol, ethanol, sodium citrate, hydrazine hydrate, ascorbate, and elemental hydrogen (Jamkhande et al., 2019; Vijayaraghavan & Ashokkumar, 2017).

Microemulsion process

This takes place in the aqueous nuclei of inverse micelles that are dispersed in an organic solvent and stabilized with a surfactant. The dimensions of these aqueous nuclei are in the nano regime and, as such, are referred to as nanoreactors. The product obtained through the reaction is homogeneous. This is one of the versatile and reproducible methods that allow the control of particle properties such as: size, morphology, geometry, homogeneity, and surface area (Vijayaraghavan & Ashokkumar, 2017).

Thermal decomposition

This is one of the most common chemical techniques for producing stable monodisperse suspensions with the ability of self-assembly. The nucleation occurs when the metal precursor is added to a heated solution in the presence of a surfactant. Meanwhile the growth phase takes place at a higher reaction temperature. The composition and size of the formed particles depend on parameters such as the reaction time, temperature, and the length of the surfactant molecule (Vijayaraghavan & Ashokkumar, 2017).

Sol-gel technique

This technique involves one of the following: 1) a mixture of preformed metallic colloids (oxides) in a sol which contains the shaping type of the matrix followed by the formation of gel; 2) the direct mix of metal/metal oxide or nanoparticles inside a sol made of pre-hydrolysed silica or 3) the complexation of metal with silone and the reduction of the metal before hydrolysis. In this method, a network formation is introduced using colloidal suspension (sol) and gelatin to form a network in a continuous liquid phase (gel). Initially, a homogenous solution of one or more selected alkoxide is prepared. A catalyst is added in order to start a reaction at a controlled pH. The formation of sol-gel involves four main steps: hydrolysis, condensation, particle growth, and particle build-up (Jamkhande et al., 2019).

Solvothermal method

This is used for the preparation of nano-phases in the presence of water or other organic chemicals such as methanol, ethanol, and polyol and solvents. The reaction is produced in a container at a pressure that allows the solvent (water and alcohol) to heat up above their boiling temperature. The crystallisation kinetic (formation of crystals) can be increased by one or two orders of magnitude through the employment of reactions assisted by microwaves (solvothermy by microwaves) (Jamkhande et al., 2019).

Electrochemical deposition

Electricity is used as a controlling force. The method consists of passing an electrical current between two electrodes separated by an electrolyte, and the synthesis of nanoparticles is produced in the electrode / electrolyte interface. The size of the particles can be controlled by changing the current density (Vijayaraghavan & Ashokkumar, 2017).

When done well, the chemical and physical processes offer greater control over the size and shape of the obtained nanoparticles. Generally, their disadvantages lie in the use of toxic chemicals on their surfaces, the use of non-polar solvents, expensive equipment that requires a high consumption of energy, and the low capacity for scaling in production.

3. Bioreduction of metallic ions and approach on green chemistry

Owing to the impact of nanomaterial synthesis on the environment generated by the use of physical and chemical methods, it has been sought to develop more environmentally friendly means of synthesis that are also consistent with the principles of green chemistry. This is why biological methods involving the reduction of metallic ions using extracts or live biological mass have been investigated, such as sources of reducers, equally so with those that are intracellular and extracellular (Agarwal et al., 2017; Carrillo-Inungaray et al., 2018; Kharissova et al., 2013; Nasrollahzadeh et al., 2020).

The intracellular processes take place within the cell. No previous treatment is required because the process is based on metabolic pathways that are probably responsible for synthesis, such as photosynthesis, respiration, and nitrogen fixation (A. Sharma et al., 2015). Diatom algae from the genera *Chaetoceros sp*., *Skeletonema sp.*, and *Thalassiosira sp.* are among the most used microorganisms (Mishra et al., 2020).

Extracellular processes are referred to as the processes that take place outside the cells, mainly supported by the exudates of cellular metabolism that comprise metabolites, ions, pigments, many proteins (enzymes) and non-protein entities such as DNA, RNA, microbial subproducts (hormones, antioxidants) and lipids (Khanna et al., 2019).

Biosynthesis methods surpass other classic procedures thanks to their advantages - the wide availability of biological entities, ecological procedures, cost-effectiveness and easy scaling (Jamkhande et al., 2019; Kuppusamy et al., 2016). Bacteria, fungi, yeasts, algae, and plants are among the different organisms that are used.

3.1 Bacteria

Prokaryotes have gained attention as a means of synthesis for metallic NPs owing to their abundance in the atmosphere and their capacity to adopt extreme conditions. Their advantages relate to their rapid multiplication - some well-known species are easy to grow and manipulate. However, regarding their disadvantages, it stands out that the detection of suitable microbes is a process that requires a lot of time. A careful control of both the cultivation method and the whole process is necessary in order to avoid contamination. This is combined with the lack of control regarding the size and shape of the NPs and the associated cost of the means used to grow bacteria (Agarwal et al., 2017; Jamkhande et al., 2019). Saravanan et al. (2021) report investigations with the genera *Pseudomonas*, *Bacillus*, *Streptomyces*, *Escherichia*, *Aeromonas*, *Enterobacter*, and *Klebsiella* used for the reduction of Ag, Au, ZnO, Cu and Cd NPs. On the other hand, Yusof et al. (2020) used cellular biomass and supernatant from *Lactobacillus plantarum* in order to obtain ZnO NPs ranging between 191.8-291.1 nm in size. Joshi et al. (2018) used *Geobacter sulfurreducens* with the goal of obtaining Fe NPs with magnetic properties. The process produced a mineral phase of Fe(II) with similar characteristics to magnetite, due to which the authors suggested that these nanoparticles could be used for the cleaning of soils contaminated with other metals. For obtaining Au NPs, *Rhodopseudomonas capsulata* (He et al., 2007), *Deinococcus radiodurans* (Li et al., 2016), *Shewanella oneidensis* y *Shewanella xiamenensis* (Wu & Ng, 2017) have been tried.

3.2 Fungi

The extracellular synthesis of NPs through fungi is very useful owing to the great scale of production and the economic viability. In this case, the enzymes and proteins secreted by the fungi work as reducing agents, allowing the synthesis through metallic salts. The fungi variants are chosen over bacteria owing to their greater tolerance and bioaccumulation of metals, as well as their capacity to reduce great quantities of NPs (Agarwal et al., 2017; Jamkhande et al., 2019; Singh et al., 2018). *Aspergillus* is among the commonly implemented genera, Ninganagouda et al. (2013) used the species *A. flavus* for the extracellular reduction of Ag, from which they evaluated its antimicrobial activity against *Pseudomonas aeruginosa*, *Escherichia coli* and *Klebsiella pneumonia*, with effective results. *A. niger* has also been used for the reduction ZnO (Kalpana et al., 2018), as well as *A. fumigatus* for the biosynthesis of CuO (Ghareib et al., 2019). In both cases, the objective was to use the obtained NPs for photocatalytic processes in the removal of ZnO, as well as evaluating its catalytic activity in organic synthesis (Shamsuzzaman et al., 2017). In this sense, through their study, Ovais et al. (2018) emphasize some works in which various genera have been used for the reduction of NPs. In the case of intracellular biosynthesis, *Aureobasidium*, *Fusarium*, and *Rhizopus* have been used for gold and silver NPs; for the extracellular processes, the *Candida* and *Aspergillus* genera have been worked with for the reduction of Ag, ZnO, and Co.

3.3 Algae

Algae are photosynthetic organisms that vary from unicellular types (*Chlorella*) to multicellular types (kelps). They lack basic vegetal structures like roots and leaves and are classified according to the pigment present inside them, such as the red pigment in Rhodophyta, the brown pigment in Phaeophyta, and the green pigment in Chlorophyta (Agarwal et al., 2017). They are considered to be potential sources of a broad group of secondary metabolites, proteins, and pigments with which they can serve as nano factories of metallic nanoparticles (Khanna et al., 2019). Some implemented species are *Macrocystis pyrifera* for the reduction of CuO NPs (Araya-Castro et al., 2021), *Botryococcus braunii* in obtaining Cu, Ag, Pt and Pd NPs (Arya et al., 2018, 2020), *Chlamydomonas reinhardtii* for Cu NPs (Žvab et al., 2021), whilst Salem & Funda (2020) report in their evaluation that species from the genera *Chlorella*, *Phaeodactulum*, *Sargassum* and *Shewanella* have been used for the reduction of Au, Cd, and Pt NPs.

4. Biosynthesis of nanoparticles of metallic ions using plants

Compared with the synthesis of nanoparticles mediated by microorganisms, the use of plants presents diverse advantages owing to the rich biodiversity and easy availability of vegetative organisms that have been explored for the synthesis of nanomaterials (Kuppusamy et al., 2016).

They also represent less biological risks during production and eliminate the laborious process of cell cultivation, which has led to plants being considered the better option to reduce metallic ions, as well as being ideal candidates for the production on a great scale. This is in addition to producing stable NPs which are variable in both size and shape (Agarwal et al., 2017; Gan & Li, 2012; Nasrollahzadeh et al., 2020).

The metallic ions are biologically reduced to zero-valent metals or particles of metal oxide due to the phytochemicals present in the plant extracts constituted by their primary and secondary metabolites. They participate in a constant way in the redox reaction of their metabolic pathways, and act as reducing agents and stabilizers, minimizing the agglomeration and oxidation of nanoparticles. In addition, the process is generally carried out aqueously, thus dispensing with other organic solvents, and as such reducing the generation of toxic waste (Agarwal et al., 2017; Gan & Li, 2012; Jamkhande et al., 2019; Nasrollahzadeh et al., 2020). In accordance with Agarwal et al. (2017), pigments, terpenoids, flavonoids, alkaloids, carbonyls, amide groups, amines, phenols, vitamins, and amino acids are among the main reducing groups, whilst the groups that work as stabilizers are carboxylic, phenolic acid, and ascorbic acid.

4.1 Phytochemicals present in vegetal extract

Flavonoids, terpene, sugars, and secondary metabolites are among the main phytochemicals responsible for the reduction of metallic ions. Some examples are shown in figure 5.1 (Singh et al., 2018).

Flavonoids are a wide group of polyphenolic compounds that are soluble in water. They comprise various classes such as flavonols, isoflavonols, anthocyanins, chalcones, flavones and flavonoids, with the capacity to actively chelate metallic ions and reduce them to nanoparticles. It has been proposed that they are the main component of the aqueous extract in most plants (Gan & Li, 2012). Flavonoids contain various functional groups capable of forming NPs. It has been postulated that the tautomeric transformation of flavonoids, from the -enol shape to the -ceto shape can release an atom of reactive hydrogen capable of reducing to metallic iron. For example, quercetin is a flavonoid with very strong chelating activity, owing to its ability to chelate in three different positions involving carbonyl and hydroxyl group in the C3 and C5 positions, and the catechol group in the C3’ and C4’ locations (Makarov et al., 2014; Singh et al., 2018).

Terpenoids are a group of diverse organic polymers, made up of units of five carbon isoprenes with strong antioxidant activity. They are commonly found in essential oils from diverse medicinal plants (Makarov et al., 2014). The sugars present in the vegetal extract have also been shown to be responsible for the formation of NPs. Monosaccharides such as glucose and fructose can act like antioxidants when they have suffered a tautomeric transformation from ketone to aldehyde. The reducing capacity of disaccharides and polysaccharides depends on the capacity on whichever of their individual components in order to adopt a form of open chain within an oligomer and providing the metallic ion access to an aldehyde group (Makarov et al., 2014; Singh et al., 2018).

In addition, amino acids and proteins have also shown the capacity to reduce. Firstly, it has been observed that this varies between different amino acids. For example, in tyrosine, the hydroxyl groups are responsible for the reduction, whilst for glutamine and asparagine, it’s the carbonyl groups. In the case of proteins, their reducing capacity and even their size, shape, and quantity of NPs will depend on the sequence of amino acids that composes them, and the access that the metallic ion has to the molecule’s reducing location (Makarov et al., 2014).

All these phytochemicals are found distributed throughout the body of the plant, which is to say in roots, stems, leaves, flowers, fruits, and seeds. This has allowed all organs to be used for the bioreduction of many metals, as can be seen in table 5.1 (Agarwal et al., 2017).

Figure 5.1 Examples of phytochemicals present in plants: a) Quercithin (flavonium); b) Gallic acid (phenolic compound); c) Geraniol (terpenoid); d) Retinol (vitamins); e) L-lysine (amino acid); f) Carotenoid (pigment).

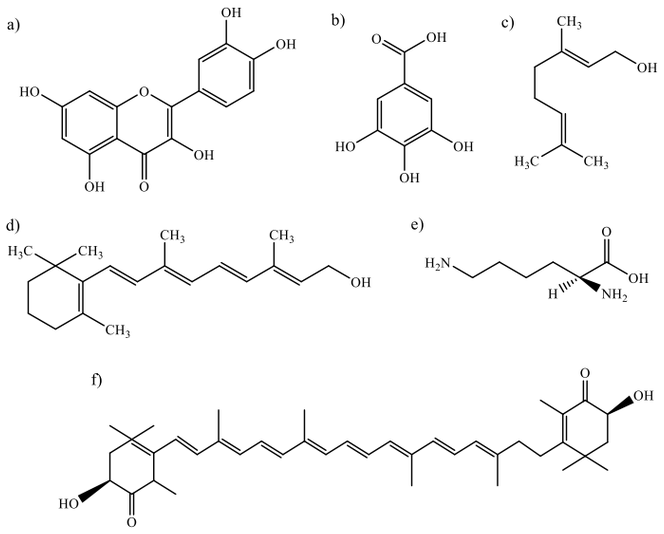

4.2 Proposed mechanisms

The elucidation of the exact mechanisms associated with the reduction of nanoparticles can be complicated - it is still not fully understood. However, some authors present certain proposals that can shed light on these mechanisms (Asghar et al., 2018).

Asghar et al. (2018) cite a possible general reaction mechanism for metallic ions in contact with phytochemicals present in vegetal extracts which could be considered for the reduction of a metal determined in equation 1:

$$nM + n(Ar - OH)n \rightarrow nM^{0}NPs + n(Ar = O) + 3nH^{+} \quad (1)$$

…where n is the number of oxidized groups for the metallic ion, M represents the metallic ion, and Ar represents the aromatic groups. The formation of NPs is confirmed by a change in pH in the solution, which decreases at the end of the reaction.

For example, Devatha et al. (2016) propose a reduction mechanism for Fe^{2+}, where they indicate that the presence of polyphenolic groups directly reduces the iron ions to zerovalent iron. This is explained through stoichiometric equation 2, where Ar represents the phenyl groups:

$$nFe^{2+} + 2Ar\text{-}(OH)n \rightarrow nFe^{0} + 2nAr = O + 2nH^{+} \quad (2)$$

Ahmad et al. (2018) report that they identified the presence of protocatechuic acid (polyphenolic compound) in the palm oil that they used for the reduction of trivalent gold in their analysis of FTIR. They mention that owing to the fact this compound was reported previously as one of the most abundant of this material, it was taken as a model compound that reacts with trivalent gold ions to oxidize by giving electrons to Au^{3+} in order to reduce them to gold atoms, as is shown in figure 5.2.

Figure 5.2 Reduction mechanism for Au^{3+} with oil palm leaves *(modified from Ahmad et al., 2018).*

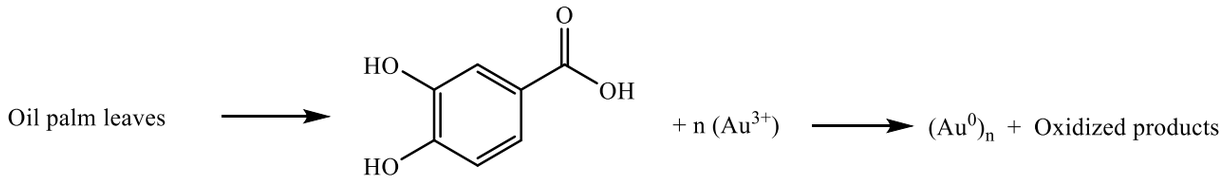

In the same way, possible mechanisms for bimetallic nanoparticles that intervene in the reduction process have been suggested. Such is the case for Olajire & Mohammed (2020), who carried out a green synthesis of Pd/Au using *Ananas comosus* leaves as a reducing agent.

They indicate that the analysis of the FTIR spectrum evidence that reduction of the ion mix is predominantly carried out by O-H groups of polyphenolic compounds, one of the isolated bioactive compounds of the leaf extract. For this reason, they propose a reaction mechanism between the polyphenolic compound and the mixture of palladium/gold ions (Pd^{2+}-Au^{3+}), where the electrons are given by the polyphenolic compound to the vacant d orbital of the mixture of palladium/gold ions, and later they are converted into a palladium atom (Pd^0) - gold atom (Au^0) (Fig 5.3). It is observed that through the mechanism, the π electrons of the polyphenol aromatic ring can transfer electrons to the vacant d orbital of the palladium-gold ions and convert them into free atoms.

Figure 5.3 Proposed mechanism for bioreduction of the ions mixture Pd^{2+} y Au^{3+} a Pd y Au with polyphenolic compounds in *A. comosus (modified from Olajire & Mohammed, 2020)*

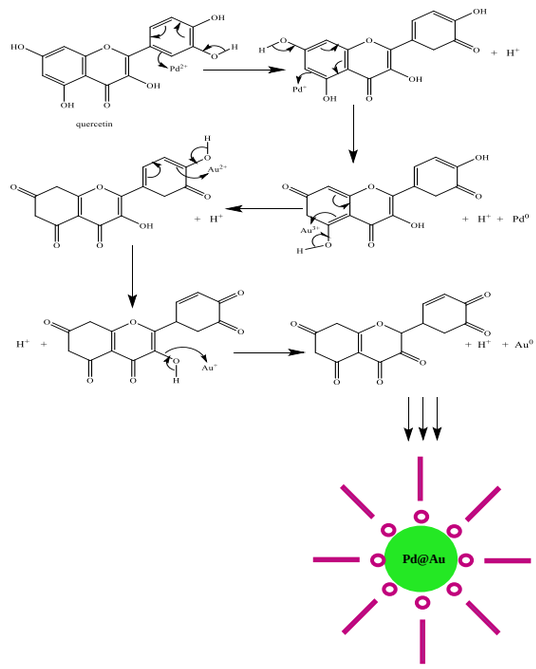

Table 5.1 Bioreduction of metallic particles using plants

Metal	Reducing agent	Plant organ	Chemical species obtained	Form	Average diameter (nm)	UV-Vis (λ_{max}) nm	Functional groups	Applications	Author, year.
Ag	*Artemisia annua* L.	Leaves	Ag^0	Spherical	49.4 - 88	400- 500	ND	Antibacterial activity	(Aghajanyan et al., 2020)
	Azadirachta indica	Leaves	Ag^0	Spherical	34	436- 446	N-H amines C=O alkyl groups C-O, C-OC- flavonoids and terpenoids	Antibacterial activity	(Ahmed et al., 2016)
	Salvia officinalis	Leaves	Ag^0	Spherical	40	439- 446	C=O, O-H, N-H phenolic compounds, flavonoids, proteins and saponins.	Dye removal	(Albeladi et al., 2020)
	Commiphora myrrh	Resin	Ag^0	Spherical	22	445	O-H, C-H phenolic compounds.	Antibacterial activity	(Alwhibi et al., 2020)
	Green tea Black tea	Leaves	Ag^0	Spherical	10 -20	ND	O-H, C-H y C-O-H phenolic compounds.	Antibacterial activity	(Asghar et al., 2018)
	Lippia citriodora	Leaves	Ag^0	Spherical	14	430	C-O, O-H, C=C phenolic compounds.	Medical activity	(Cruz et al., 2010)
	Acalypha wilkesiana	Leaves	Ag^0	Spherical	10 -26	450	O-H, C-H, C=C phenols, terpenoids, saponins and flavonoids.	Antibacterial activity	(Dada et al., 2019)
	Vitex sp.	Leaves	Ag^0	Spherical	86	ND	C-H, O-H, C-O-C polyphenols	Antibacterial activity	(Deeksha et al., 2021)
	Clitorea ternatea	Flowers	Ag^0	Cubical	18 -50	400- 450	C-CH phenols and anthocyanins C=O y OH phenolic compounds.	Antibacterial activity	(Fatimah et al., 2020)
	Acanthe phylum bracteatum Persian manna	ND	Ag^0	Spherical	40	425	ND	ND	(Forough & Farhadi, 2010)
	Nelumbo nucifera	Flowers	Ag^0	ND	90	450	N-H, C-C, C-O aromatic groups, alcohol	ND	(Hitesh & Lata, 2018)
	Anthurium andraeanum	Leaves	Ag^0	Spherical	12- 46	419	ND	Antibacterial activity	(Korkmaz, 2020)
	Ocimum sanctum	Leaves	Ag^0	Spherical	3- 20	436	O-H alcohols, polyphenols, carboxylic acids. C-N aromatic amines N-H primary amines	ND	(Mallikarjuna et al., 2011)
	Prunus domestica	Fruit	Ag^0	Spherical	50	380- 450	C-N, N-H amines C-H, O-H carboxylic acids and aldehydes	ND	(Mohaghegh et al., 2020)
	Catharanthus roseus	Leaves	Ag^0	Spherical	48- 67	440	ND	Antibacterial activity	(Mukunthan et al., 2011)
	Allium sativum L. *Camellia sinensis* L. *Curcuma longa* L.	Slice Leaves Rhizome	Ag^0	Spherical	8.19 8.37 6.13	447- 451	OH, C-H, C-N, N-H phenolic compounds, flavonoids, proteins, sugars.	Antioxidant and cytotoxic activity.	(Selvan et al., 2018)
	Terminalia bellerica	Grain	Ag^0	Spherical	29.6	350- 450	-NH_2, -OH proteins, C=O terpenoids or other aromatic groups. C-O-C proteins or saccharides.	Catalytic activity	(Sherin et al., 2020)
	Olea europaea	Fruit	Ag^0	Spherical	11.6- 20.7	436	O-H, N-H, CO-O-CO alcohols, phenols and proteins.	Antimicrobial activity	(Umai et al., 2020)
	Phyllostachys aurea	Leaves	Ag^0	Spherical	13 ± 3.5	420- 450	ND	Antibacterial activity	(Yasin et al., 2013)
Au	*Elaeis guineensis*	Leaves	Au^0	Spherical	27.89 ± 14.59	500- 550	O-H polyphenolic compounds, C=O y N-H proteins and carboxylic acids C-N, C-O phenolic compounds and amines.	ND	(Ahmad et al., 2018)
	Jasminum auriculatum	Leaves	Au^0	Spherical	8 - 37	547	O-H, C=O, N-H flavonoids, terpenoids, alkaloids and polyalcohols.	Catalytic and antibacterial activity	(Balasubramanian et al., 2020)
	Citrullis lanatus	Fruit	Au^0	Spherical, hexagonal, and triangular	100- 200	560	ND	Antibacterial activity	(Chamsa-ard et al., 2019)

Metal	Reducing agent	Plant organ	Chemical species obtained	Form	Average diameter (nm)	UV-Vis (λ_{max}) nm	Functional groups	Applications	Author, year.
	Vitis vinifera L.	Fruit	Au^0	Spherical	57.1 ± 16.4	550.6	C=O, C=C, O-H phenolic compounds, carboxylic acids.	ND	(Dzimitrowicz et al., 2018)
	Gnidia glauca	Flowers	Au^0	Spherical, triangular and prism	5- 20	540	O-H, C=C, N-H, phenols, alcohols	Catalytic activity	(Ghosh et al., 2012)
	Coleus amboinicus	Leaves	Au^0	Spherical, triangular, and hexagonal	20.5 ± 11.45	536	C-N Aromatic amines, C-OH secondary alcohols	ND	(Narayanan & Sakthivel, 2010a)
	Camellia sinensis	Leaves	Au^0	Spherical, triangular y hexagonal	18	536 529 (24 h)	Confirm the presence of polyphenols	Metal ion sensor	(Silva-De Hoyos et al., 2019)
	Citrus paradisi	Fruit	Au^0	Spherical Triangular and hexagonal	10- 90 75- 325	540- 568	O-H, C-H, C=O, C-O-C polysaccharides	Metal ion sensor	(Silva-De Hoyos et al., 2020)
	Gymnocladus assamicus	Scabbard	Au^0	Hexagonal, pentagonal and triangular	13.31 ± 2.5	526	ND	Catalytic activity	(Tamuly et al., 2013)
	Aegle marmelos, *Eugenia jambolan* *Annona muricata*	Fruits	Au^0	Cubical	18 16 28	519 523 526	C=O, N-H, O-H, aromatic compounds.	Anticancer activity	(Vijayakumar, 2019)
	Muntingia calabura L.	Leaves	Au^0	ND	36.93	543.5	O-H, C=O flavonoids, tannins, terpenoids, C-N, C-H proteins.	ND	(Wahab et al., 2018)
	Phoenix dactylifera L.	Leaves	Au^0	Spherical	32- 45	552	C=O, O-H carbohydrates, tannins, flavonoids, phenolic acids.	Catalytic activity	(Zayed & Eisa, 2014)
Fe	Neem Mango Rose Clove Carom	Leaves Leaves Leaves Buds Seeds	Fe_3O_4 y α-Fe Fe_3O_4 y α-Fe Fe_2O_3, Fe_3O_4 y α-Fe Fe_2O_3, Fe_3O_4 y α-Fe α-Fe	Spherical Spherical Spherical Spherical Spherical	Micro/nano	320- 325 470- 475	C=C alkene groups -PH phosphines. N-H secondary amines. C-O-C, C=O polysaccharides, nucleic acids, and proteins	ND	(Afsheen et al., 2018)
	Green tea	Leaves	α-Fe_2O_3	Spherical	40 -80	570	ND	Photocatalytic activity	(Ahmmad et al., 2013)
	Green tea Black tea	Leaves	Fe^0	Spherical	42- 60	ND	C-OH, C=C, C-O-C flavonoids.	Antibacterial activity	(Asghar et al., 2018)
	Green tea	Leaves	FeO	Quasi-spherical	25.5 ± 0.6	270	ND	Dye removal	(De León-Condés et al., 2019)
	Magnifera indica *Murraya koenigii* *Azadiracta indica* *Magnolia champaca*	Leaves Leaves	Fe^0 Fe^0 Fe^0 Fe^0	Spherical Spherical Spherical Spherical	100- 150 100- 150 96- 110 99- 129	216- 256 256- 277 296- 325 259- 282	O-H, C-H, C-H_2 phenolic and aliphatic compounds	Domestic wastewater treatment	(Devatha et al., 2016)
	Green tea Oolong tea Black tea	Leaves	α-Fe, Fe_2O_3, Fe_3O_4 y FeOOH	Spherical	40- 50	500- 700	ND	Dye removal	(Huang et al., 2014)
	Moringa oleifera (MOS) (MOL)	Seeds Leaves	Fe^0	Spherical	2.6- 6.2 3.4- 7.4	210- 240	O-H, N-H, C-O, C-H, C= proteins and fatty acids O-H, C-H, C=O amino acids, flavonoids, phenolic compounds.	Nitrate removal and antibacterial activity	(Katata-Seru et al., 2018)
	Eucalyptus sp.	Leaves	FeNPs RGO/FeNPs	Spherical	4- 7	330- 450 270 y 330- 450	C-O, C-C, C=O graphene groups, characteristic groups of eucalyptus were identified.	Adsorbent activity	(X. Weng et al., 2018)
Cu	Green tea Black tea	Leaves	Cu^0	Spherical	26- 40	ND	C-H, O-H flavonoids, and phenolic compounds -OH, C-O-C phenolic groups	Antibacterial activity	(Asghar et al., 2018)
	Punica granatum	Fruit shell	CuO	Spherical	10- 100	282	O-H, N-H phenolic groups and alcohols, C=C, C=O, C-OH, C-N proteins.	Insecticide	(Ghidan et al., 2016)
	Azadirachta indica	Flowers	Cu^0	Spherical	44.9	560	N-H, C=O, C-OH terpenes, proteins.	Antibacterial activity	(Gopalakrishnan & Muniraj, 2019)
	Eucalyptus globulus L. *Mentha piperita*	Leaves Leaves	Cu^0 Cu^0	Triangular Cluster	60- 75 36- 50	ND	ND	Antifungal activity (Phytopathogens)	(Iliger et al., 2021)
	Ziziphus spina-christi	Fruit	Cu^{2+} y Cu^+	Spherical	5- 20	551	C-H, -NH, -OH, C=O phenols, alcohols, carboxylic groups.	Dye removal and antibacterial activity	(Khani et al., 2018)
	Abies spectabilis	Aerial parts	CuO	Spherical	50	403	C-O-C, C-O, C=O y OH	Anti-inflammatory and contraceptive activity	(Liu et al., 2020)
	Azadirachta indica	Leaves	Cu^0	Cubical	48	560	O-H phenolic groups C-N aromatic amines C-H Aldehydes	ND	(Nagar & Devra, 2018)
	Syzygium aromaticum	Buds	Cu^0	Spherical	15	580	C-H, C-N secondary amines, -C=C-, C=O proteins.	Antimicrobial activity	(Rajesh et al., 2018)
	Calotropis procera	Leaves	CuO	Cylindrical	40	292 y 355	O-H adsorbed on the NPs	ND	(Reddy, 2017)
	Bauhinia tomentosa	Leaves	CuO	Spherical	22- 40	384	C-H, C=O, N-O, C-O phenolic groups, tannins, and proteins.	Antibacterial activity	(Sharmila et al., 2018)
	Achras sapota Linn.	Fruit	Cu^0	Spherical	20 -40	603	OH, C-H, -C=C aromatic groups.	Cytotoxic activity	(Thakore et al., 2019)
Zn	*Delonix regia*	Leaves	ZnO	Hexagonal and different superstructures	20	312	C=C, C-N, C-O amino acids, heterocyclic compounds.	Antibacterial activity, with anticancer potential.	(Begum et al., 2020)
	Medicago sativa	Leaves	Zn^0	Hexagonal	2- 5.6	335	ND	ND	(Canizal et al., 2006)
	Costus İgneus	Leaves	ZnO	Spherical	31	210 -230	ND	ND	(Chinnasamy et al., 2018)
	Jatropha sp.	Latex	ZnO	Hexagonal	100	310- 365	ND	Semiconductor	(Geetha et al., 2016)
	Nyctanthes arbor-tristis	Flowers	ZnO	Hexagonal	12-32	365- 369	N-H, C=O, C-N, C-H aromatic groups, amines and alkynes.	Antifungal activity	(Jamdagni et al., 2018)
	Moringa oleifera	Leaves	ZnO	Spherical	6- 10	350- 380	O-H, NH_2, H_3CO, C-H, OH-C=O bioactive compounds.	Electrochemical activity	(Matinise et al., 2017)
	Lycopersicon esculentum *Citrus sinensis* *Citrus paradisi* *Citrus aurantifolia*	Fruits shell	ZnO	Polyhedral	9.7 ± 3	ND	Aromatic rings.	Photocatalytic activity	(Nava et al., 2017)
	Passiflora caerulea	Leaves	ZnO	Spherical	70	380	OH, C=C, C=O, C-N polyphenols, proteins, C-O, C-N, C-H amino acids, N-H amide groups.	Antimicrobial activity	(Santhoshkumar et al., 2017)
	Eucalyptus globulus	Leaves	ZnO	Spherical	11.6	361	O-H polyphenols, C-O carboxylic acids.	Photocatalytic activity	(Siripireddy & Mandal, 2017)
	Scutellaria baicalensis	Roots	ZnO	Spherical and irregular	33.14- 99.03	316	C-H, N-H aliphatic amines and amides, -CH aromatic groups.	Antioxidant activity	(Tettey & Shin, 2019)
	Atalantia monophylla	Leaves	ZnO	Spherical	30	352	C-O, C-H, -OH proteins, N≡O, N-O, C-N aromatic amines.	Antimicrobial activity	(Vijayakumar et al., 2018)

Own Elaboration

5. Influential parameters for obtaining nanoparticles

Different factors such as pH, temperature, concentration of metal salts, or the quantity of vegetal extract, play an important role in the control of nucleation, formation, and stabilization of NPs. Changes in these parameters can induce changes in the size and shape, as well as preventing the agglomeration of NPs (Khanna et al., 2019; Rai & Yadav, 2013).

5.1 Concentration of metallic ions

In the optimization studies of Ghosh et al. (2012), for the reduction of Au with *Gnidia glauca* flowers, they found that a concentration of 0.7 mM facilitates the synthesis best in comparison to other concentrations.

They tried variations from 0.1 mM to 5 mM and found that although the synthesis speed increases with the concentration up to a value of 1 mM, in higher concentrations a reduction reaction is no longer observed. As such they conclude that this parameter plays an important role in the process. Ahmed et al. (2016) carried out green synthesis of silver nanoparticles through silver nitrate. For its optimization, they evaluated the concentration of the metallic salt from 1mM to 5mM, in accordance with the absorption spectrums obtained through UV-vis. As the concentration increases, so too does the absorption of the band locate at 445 nm. Jamdagni et al. (2018) used different concentrations of zinc acetate in order to optimize the synthesis of ZnO NPs with *Nyctanthes arbor-tristis*. They observed that an increase in the concentration of 0.0025 M to 0.01 M generates an increase in the absorption accompanied by a constriction of the band. Upon increasing to 0.02 M, a decrease in and broadening of the band absorption are generated. The investigators concluded that the increase in ion concentration beyond the threshold value leads to a decrease in nanoparticle synthesis.

In accordance with that reported by Chinnasamy et al. (2018), for the synthesis of ZnO nanoparticles with insulin plants. Through an ANOVA analysis, they found that the concentration of the metallic salt, in the case of zinc nitrate, has a greater contribution in determining the size of NPs compared to other considered parameters, such as reaction time, temperature, and quantity of vegetal extract. In this sense the studies carried out by Nagar & Devra (2018) on the optimum concentration of Cu salts indicate that upon increasing the concentration from 6mM to 7.5mM, the size of the NPs decreases. This is, according to the authors, due to the fact that the generation of NPs occurs in two steps - firstly, the nuclei are generated, and then the NPs grow. Increasing the concentration allowed the fast generation of nuclei that grew slowly, obtaining smaller nanoparticles. However, upon adding an excessive concentration of precursor salt, the high generation of nuclei will, as a result, give a greater agglomeration, increasing the final size of the NPs.

Dada et al. (2019) carried out the optimization of the synthesis process for obtaining Ag NPs with *Acalypha wilkesiana*, varying the molar concentration of the metallic salt. They found that in higher concentrations, the increase in size of the particles increases the intensity of the spectrum of the plasmon. Gopalakrishnan & Muniraj (2019) did something similar with the green reduction of copper with *Azadirachta indica* (Neem flower) trying concentrations of metal salts from 1mM to 10 mM. The optimal condition, determined by the maximum absorbance intensity of the SPR was 2mM - with higher concentrations the absorbance band begins to decrease.

5.2 Vegetal Extract

The formation of nanoparticles occurs through ionic or electrostatic interactions between the complex metals and functional groups at the surface of the biomass. It has been observed that many phytochemicals in plants are involved as reducing or protective agents during the formation of nanoparticles, and that their concentrations are critical to the way in which the process is directed (Gan & Li, 2012).

The surface chemical is one of the main factors that not only determines the activity of NPs but also plays an important role in its stability. Phenolic compounds that cover biogenic metallic nanoparticles confer them greater stability in comparison with other used reducing agents. In general, phytochemicals are adsorbed on the surface of the particles through various mechanisms. The assemblage pattern on the surface of the metal depends on various intermolecular interactions between the adsorbed molecules and the surface of the metal (Amini, 2019). It is believed that one of the adsorption mechanisms is attributable to the presence of π electrons and carbonyl groups in the molecular structures of phytochemicals (Gan & Li, 2012).

It is the availability of reducing and protective agents that determines if the metal precursors are able to reduce and eventually lead to the formation of nanoparticles. Thus, the concentration of vegetal biomass used during biosynthesis should not be overlooked, as it determines the grade of reduction and stabilization exercised by the biomolecules, which could affect the resulting size and shape of the nanoparticles (Gan & Li, 2012).

Cruz et al. (2010) evaluated the quantity of added vegetal extract for the reduction of Ag with *L. citriodora* and observed that this influences the formation of NPs. Upon analysing the absorbance spectrums in UV-vis of the SPR, they observed an increase when they increased the quantity of used vegetal extract. However, when carrying out the analysis of the size and shape of the nanoparticles through TEM, they conclude that there is not a change in these characteristics related to the quantity of vegetal extract. Gan & Li (2012) propose in their revision that when the concentration of the vegetal extract increases, so too does the electron density such as charged groups in the reducers. This would limit the free electrons of the metal cluster within a small volume and would increase the surface charges of the metal clusters in a way that makes the resulting surface charges exercise a repulsive force that could lead to a reduction in the size of the particles.

In the green synthesis of silver carried out by Ahmed et al. (2016), for the evaluation of the vegetal extract as a reducing agent, they tried quantities from 1 to 5 mL. They observed through monitoring with UV-vis that upon increasing it to 4 mL, a slight movement from 445 to 448 nm is observed, which in accordance with the authors means there is a change in the size of the particles. In a similar way, Agarwal et al. (2017) relayed that in accordance with the revised documents, when the quantity of vegetal extract is increased, the size of the NPs decreases.

In 2018, Nagar & Devra carried out the green reduction of copper with *A. indica* leaves. In order to obtain the optimal conditions for reduction, they evaluated distinct percentages of vegetal extract from 5% to 25%. They observed that with the lowest percentage, they obtained a weak absorption band of the SPR through UV-vis, whilst at 20%, the band intensity increased, which they suggest is related to the reaction speed. They corroborated this through a graph of the conversion rate versus the vegetal extract percentage - the results indicate that the conversion rate increases with the increase of the extract percentage up to 20%. With higher percentages than this, the speed remains constant, which indicates agglomeration of the NPs. This is due to the excess of present biomolecules that promote a secondary reduction process, which begins on the surface of the performed nuclei, which increases the size of the NPs. Jamdagni et al. (2018) evaluated the influence of the quantity of flower extract from *Nyctanthes arbor-tristis* added to the synthesis of ZnO. They determined that an increase from 0.25 to 1 ml of extract in 50 mL of metal solution improves the absorption and bandwidth, whilst any increase or decrease of this volume generates a decrease in the absorption and bandwidth, and thus decreases the synthesis of NPs. On the other hand, Gopalakrishnan & Muniraj (2019) report in their optimization of the process that they evaluated different volumes of vegetal extract for the reduction of copper through the Neem flower, from 8 to 12 mL. They found the optimum volume was achieved at 10 mL, which signals that the results were based on the maximum absorption intensity of the band of the SPR found at a wavelength of 560 nm.

5.3 pH

Various investigations have shown that the size and shape of biosynthesized nanoparticles can be manipulated by varying the pH of the reaction mixtures (Rai & Yadav, 2013). An important influence of the pH of the reaction is its capacity to change the electric charge of the biomolecules, which could affect its stabilizing capacity and, subsequently, the growth of NPs. This could result in the favorable formation of certain shapes in a particular pH range in a way that could achieve a greater stability (Gan & Y 2012).

Nagar y Devra (2018) evaluated the synthesis of copper through *A. indica*. The authors considered the optimization of different factors to be important for their reduction process, among which was pH. They observed that for acidic values (4.5) the reduction reaction didn't occur, probably due to the inactivation of the involved biomolecules. For a high pH (6.6), small NPs were produced, whilst at higher pHs, the generation of bigger sized NPs was observed, which suggests an agglomeration process. The authors also report that during the synthesis process, the pH decreases owing to the release of H^+ ions on the part of the species in the extract due to their oxidation in the presence of Cu^{2+} ions. Dada et al. (2019) investigated the effect of the pH on the formation speed of Au NPs and found that it increases when the pH is increased to 9.0. They propose that this is due to the responsible OH groups of the reduction, and that the formation of silver nanoparticles is more favorable in basic means corroborated by the SPR obtained through basic means.

Aghajanyan et al. (2020) evaluated the effect of pH on the synthesis of Au using *Artemisia annua*. They observed that the formation of smaller spherical NPs is favored in neutral and alkaline pH (7.0, 9.0). They evaluated the values of acidic pH (3.0, 5.0) in the same way, and did not observe the formation of NPs. In a similar way, Gopalakrishnan & Muniraj (2019), in optimizing the pH value for obtaining copper nanoparticles, signal that the most favorable pH was 9.0, having evaluated pH values from 8.0 to 12.0. Jamdagni et al. (2018) also evaluated the optimum pH for the reduction to ZnO. The evaluated values varied from 9.0 to 13.0 - the lowest values did not show the formation of NPs, whilst with 12.0 and 13.0, the characteristic absorption band was observed. However, the band obtained at pH 12.0 was the clearest, and as such this value was considered the most suitable for the reduction.

5.4 Temperature

The temperature is considered to be a crucial factor in the formation of NPs, affecting the process of nucleation and their size. Cruz et al. (2010) report the evaluation of two temperatures used in the reduction of Ag with *L. citriodora* of 25 and 95°C. The results through UV-vis showed that upon increasing the temperature, a displacement in the absorption band of 440 to 420 is given. They also observed that the band of 440 nm obtained at 25°C modifies itself 24 h after the reaction, reaching 420 nm, whilst with the temperature at 95°C, both the intensity and the maximum length of the absorption band remain constant. The analyses with a transmission electron microscope suggest that this decrease in wavelength is related to the distribution of the size of the NPs. For Ghosh et al. (2012), the study of temperature optimization revealed a direct effect on the speed of the reaction kinetic for gold NPs. They observed that low temperatures (0 to 20°C) do not allow synthesis, whilst at average temperatures (30 to 40°C) a moderate synthesis was observed, and at 50°C a maximum speed was found, which supports what was previously reported, which indicates that high temperatures play a key role in improving the speed of the reaction. Nagar & Devra (2018) studied the effect of temperature on the formation of copper NPs and observed that upon increasing the temperature from 60 to 85°C, the rate of conversion increases in a way in which the effect of the temperature on the nucleation speed is greater than that on the speed of growth. However, when the temperature is too high, it promotes the nuclei to be colloidal, and they agglomerate, which is why the optimum temperature is 85°C.

On the other hand, Dada et al. (2019) studied the effect of temperature on the synthesis of silver nanoparticles, for which they varied the temperature from ambient temperature to 100°C. They observed that the increase in temperature generates an increase in the intensity of the band of the plasmon as a result of the bathochromic change, which results in a decrease in average diameter of the NPs. In order to ascertain the effect that was generated in green synthesis, Aghajanyan et al. (2020) used UV-vis spectrophotometry in order to monitor the formation of the surface plasmon resonance (SPR). The spectra evidenced the formation of Ag NPs in a short time between 40 and 60°C, and although they observed the formation of NPs at ambient temperature, this was slower, and the absorption band generated by SPR was not as pronounced as at the higher temperatures. Moreover, Gopalakrishnan & Muniraj (2019) also tested temperatures of 35, 80, and 90°C during the optimization process for obtaining Cu NPs, reporting that 80°C was the best. In the same way, Jamdagni et al. (2018) signaled that the most suitable for the reduction of ZnO with *Nyctanthes arbor-tristis* is 90°C, as they obtained the most prominent and narrow absorption band with only this temperature.

As observed, there are no unique conditions that can apply to each metallic salt, and which generate NPs with specific characteristics. As such, carrying out an optimization process that considers the following ranges as distinct parameters is recommended. Regarding the concentration of metallic salts, it is suggested that the working concentrations be considered to be in the range of 1 to 10 mM mainly in the case of noble metals. In accordance with that revised for other metallic ions, it is possible to increase the range to 0.1 M. It is important to remember that excessive concentrations can limit the reduction, and thus generate agglomeration that can affect the characteristics that are sought in NPs. The salt precursor also proves to be important given that when dealing with a nitrogenous salt, the concentrations can be smaller. In the case of vegetal extract volume, as reported previously, upon increasing this factor, the size of the NPs decreases. As such, the use of percentages higher than 5% is recommended. For the pH, it is recommendable to work between the values of 5.0 and 12.0, given that lower values will not have a reduction process. For the temperature, it is better to work with high temperatures, or those that are at least higher than 50°C and lower than 100°C.

6. Characterization techniques

Once prepared, the metallic nanoparticles conform to diverse characterization techniques in order to determine their size, shape, distribution, morphology, and surface area. The spectroscopic and diffractographic techniques involved include UV-visible spectroscopy (UV-vis), energy dispersion spectroscopy (EDS), x-ray diffraction (XRD), Fourier-transform infrared spectroscopy (FTIR), x-ray photoelectron spectroscopy (XPS), and they are used to analyses the chemical composition, structure, and crystalline phase of NPs. On another note, microscopic techniques such as scanning electron microscopy (SEM), transmission electron microscopy (TEM), high resolution transmission electron microscopy (HR-TEM), and atomic force microscopy (AFM), are employed in order to determine the size and morphological characteristics of the NPs (Khanna et al., 2019).

Table 5.2 Characterization techniques implemented in the study of bioreduced metallic nanoparticles

NPs	UV-Vis	DRX	EDS	DLS	XPS	IR-TF	SEM	TEM	AFM	TGA	BET	Author, year
Ag	•			•				•				(Aghajanyan et al., 2020)
	•			•		•		•				(Ahmed et al., 2016)
	•	•				•		•		•		(Albeladi et al., 2020)
	•					•		•				(Alwhibi et al., 2020)
	•		•			•	•					(Asghar et al., 2018)
	•	•	•			•		•				(Cruz et al., 2010)
	•		•			•	•	•				(Dada et al., 2019)
		•				•	•					(Deeksha et al., 2021)
	•	•			•	•	•	•				(Fatimah et al., 2020)
	•	•	•				•					(Forough & Farhadi, 2010)
	•	•				•						(Hitesh & Lata, 2018)
	•	•					•	•				(Korkmaz 2020)
	•	•				•		•				(Mallikarjuna et al., 2011)
	•	•			•	•	•	•				(Mohaghegh et al., 2020)
	•		•				•					(Mukunthan et al., 2011)
	•	•	•			•	•	•				(Selvan et al., 2018)
	•	•	•			•	•	•				(Sherin et al., 2020)
	•	•	•			•	•					(Umai et al., 2020)
	•	•	•					•				(Yasin et al., 2013)
Au	•	•			•	•	•	•		•		(Ahmad et al., 20189
	•		•			•		•				(Dzimitrowicz et al., 2018)
	•	•		•		•		•				(Ghosh et al., 2012)
	•	•	•			•	•	•				(Narayanan & Sakthivel, 2010a)
	•	•	•					•				(Tamuly et al., 2013)
	•		•			•		•				(Vijayakumar, 2019)
	•	•				•	•					(Wahab et al., 2018)
Fe	•	•		•		•	•					(Afsheen et al., 2018)
	•	•			•		•	•				(Ahmmad et al., 2013)
	•		•			•	•					(Devatha et al., 2016)
	•	•	•				•				•	(Huang et al., 2014)
	•	•				•		•				(Katata-Seru et al., 2018)
	•		•		•			•				(Weng et al., 2018)
Cu	•	•				•	•					(Ghidan et al., 2016)
	•	•				•	•	•				(Gopalakrishnan & Muniraj, 2020)
		•					•	•				(Iliger et al., 2021)
	•	•				•	•	•				(Khani et al., 2018)
	•					•		•				(Liu et al., 2020)
	•	•	•			•	•	•				(Nagar & Devra, 2018)
	•	•				•		•				(Rajesh et al., 2018)
	•	•				•	•			•		(Reddy, 2017)
	•	•	•			•		•				(Sharmila et al., 2018)
Zn	•	•				•	•	•				(Begum et al., 2020)
	•	•						•				(Canizal et al., 2006)
	•	•	•			•	•					(Chinnasamy et al., 2018)
	•	•	•			•	•	•				(Geetha et al., 2016)
	•	•		•		•		•				(Jamdagni et al., 2018)
	•	•	•			•		•				(Matinise et al., 2017)
	•	•	•			•	•		•			(Santhoshkumar et al., 2017)
	•	•	•	•			•	•				(Siripireddy & Mandal, 2017)
	•		•			•	•	•				(Tettey & Shin, 2019)
	•	•	•			•	•	•				(Vijayakumar et al., 2018)

Own Elaboration

6.1 UV-vis

UV-vis spectrophotometry is employed to confirm the synthesis of NPs (Agarwal et al., 2017). Various investigators agree that one of the first signs of the reduction of metals is the change in color between the solutions before and after the reduction reaction. They mention that this change indicates the formation of nanoparticles, confirmed by the visible surface plasmon resonance (SPR) in the UV-vis absorption spectrum (Asghar et al., 2018; Kuppusamy et al., 2016). As observed in table 2, it is one the first pieces of evidence that the reaction reduction has taken place. The surface plasmon resonance for each type of particle can be found in the form of characteristics in a specific region of the absorption spectrum in a way that the SPR of silver NPs can be found between 400 to 500 nm, whilst for gold NPs, they are generally found between 500 to 550 nm, as shown in table 5.1.

SPR gives a spontaneous spectroscopic signal generated by the formation of nanostructures, which is due to the free electrons which emerge due to the conduction and valence bands being very close to each-other. When the oscillating electromagnetic field (in the light) generates a coherent collective oscillation of electrons from the conduction band of the metals during their exposure to the light, it provokes a separation of charge around the surface of the metals (Ahmad et al., 2018; Dada et al., 2019).

6.2 FTIR

Analyses through Fourier-transform infrared spectroscopy (FTIR) are relevant for determining the functional groups present in vegetal extracts, which allows the investigation of the underlying synthesis mechanism, and the surface chemical. Usually the ranges used are found between 4000 and 400 cm^{-1}, with a resolution of 4 cm^{-1}, which gives a clear idea of the reducing agents responsible for the covering, reduction, and stabilization of the NPs. The main limiting factor of this technique is found in the superposition grade of the IR absorption bands in the complex biological matrix (Dada et al., 2019; Khanna et al., 2019).

The comparison between the transmittance spectra of the aqueous vegetal extract and the means of reaction offers information on the biomolecules involved in the process (Dada et al., 2019; Khanna et al., 2019). The extracts contain numerous functional groups like C=C (alkenes), C=N (amide) O=H (phenolics and alcohol), N- H (amine), C - H and COO- (carboxylic groups).

6.3 XRD

The purity, crystalline size, geometry, orientation, and phases can be determined through XRD data. Generally, the diffraction patterns are compared with a standard crystallographic database such as JCPDS in order to have the structural information. Using the Debye Scherrer formula (3), an approximation of the particle size is obtained. XRD functions well with the identification of NPs in one or various phases. Additionally, the diffractogram is influenced by amorphous NPs that have varying interatomic longitudes (Khanna et al., 2019).

$$D = \frac{K\lambda}{\beta coscos\,\theta} \tag{3}$$

...where K is the Scherrer constant (K = 0.94), D is the average size of the crystal, β is the total width at half the maximum of the spikes (FWHM) for a Gaussian adjustment, λ corresponds to the wavelength of the used radiation Cu Kα (λ= 0.1546 nm), and θ is half of the diffraction angle of the Bragg peak (Rajesh et al., 2018).

6.4 XPS

Typically for the determination of chemical types present in a sample, an analysis through x-ray photoelectron spectroscopy (XPS) is turned to. It can also shed light on the interaction between NPs and their adjacent biomolecules, as well as signaling the presence of secondary or undesired elements that could reduce its efficiency or lead to a secondary reaction and process contamination (Ealia & Saravanakumar, 2017; Khanna et al., 2019).

6.5 SEM/TEM

Scanning electron microscopy (SEM) offers information on particles at the nanoscale and helps to determine the surface morphology and the dispersion of free NPs or those in the matrix. Transmission electron microscopy (TEM) is more commonly used for the size and shape and can also offer information on the number of layers of the material, given that it varies from a low or high increase. However, when both are combined with EDAX or EDS, information is provided on the elements present. When the precise shape, size, and crystalline structure need to be known, HR-TEM is used (Khanna et al., 2019). As has been observed, all the implemented characterization techniques provide important and necessary information regarding the characteristics of bioreduced NPs. Among these techniques, a conclusive tool for said characteristics is transmission electron microscopy. However, it is appropriate to highlight that UV-vis spectrophotometry is the first technique chosen to confirm the presence of NPs in the bioreduction solution (Powar & Patel, 2019; Vijayaraghavan & Ashokkumar, 2017).

7. Applications

Metal nanoparticles are of great interest to several disciplines including biotechnology / biomedicine, bioremediation, agriculture, catalysis, biosensors, among others (Rai & Yadav, 2013).

7.1 Monometallic Particles

Silver

According to Dada et al. (2019), of all metal nanoparticles, those of silver have been largely explored by researchers around the world due to their versatility, simplicity of synthesis, adaptability, morphology, and high surface area. One of its main applications resides in the evaluation of their antibacterial activity. In this sense, Yasin et al. (2013) obtained AgNPs with bamboo leaves through bioreduction, tested against the pathogenic bacteria *E. coli* and *Staphylococcus aureus*; the results indicate that the effectiveness of the NPs applied increases with the concentration used, however, they reported that 20 μg / mL is the minimum concentration that reduces bacterial proliferation.

Korkmaz (2020) evaluated the bactericidal activity of AgNPs obtained by green reduction with *Anthurium andraeanum* against the bacteria: *Enterobacter aerogenes*, *Salmonella infantis*, *Salmonella typhimurium*, *Escherichia coli*, *Enterococcus faecalis*, *Staphylococcus aureus*, *Staphylococcus epidermidis* and *Bacillus epidermidis*. MIC and MBC tests indicated that the minimum inhibitory concentration against all species was found at 0.125 mg / mL, while the bactericidal effect for all strains was 1 mg / mL except for *S. aureus*. Alwhibi et al. (2020), synthesized AgNPs with *Commiphora myrrha* and tested its antibacterial activity against several gram-negative strains. According with the authors, the antibacterial effectiveness is explained by two pathways, the first is membrane damage through an association / interaction of NPs with biomolecules and DNA, causing the inhibition of cell multiplication, and second by formation of reactive oxygen species through their interaction with enzymes and / or biomolecules generating cell damage or destruction. This same study concerned the anticancer activity of NPs and found that cell viability is reduced by increasing the concentration of nanoparticles used, reaching 30% cell viability with 100 μL of AgNPs.

Silver NPs have also been applied as catalysts, Albeladi et al. (2020), for example carried out the green reduction of Ag with *Salvia officinalis* and evaluated their ability to degrade the Congo red dye (CR) through a catalytic reduction with sodium borohydride ($NaBH_4$). It was found that the addition of Ag NPs significantly increase the degradation of the dye up to 82.22 % due to the high availability of active sites on their surface where electron transfer is mediated. Sherin et al. (2020), also tested the catalytic capacity of AgNPs synthesized with *Terminalia bellerica* for the degradation of four organic pollutants (4 nitrophenol, methyl blue, eosin yellow and methyl orange), the results showed good catalytic activity with the dose dependent on ambient conditions.

Gold

Gold nanoparticles are among the most used for medical applications as reported by Amini et al. (2019); their antibacterial activity was tested by Chamsa-ard et al. (2019), against *Escherichia coli* and *Staphylococcus epidermidis*, with NPs obtained by bioreduction with *Citrullis lanatus*; the fruit was split in two parts, the inner red and the outer green; each portion allowed obtaining AuNPs with outstanding antibacterial properties, which is why the authors consider that the AuNPs are potential candidates for incorporation in new types of antibiotics. Also, the authors highlighted the effectiveness of the production technique based on green chemistry and its low cost.

Balasubramanian et al. (2020), obtained AuNPs by green reduction with *Jasminum auriculatum* leaf extract and evaluated their antimicrobial activity against various species of pathogenic bacteria and fungi, the results obtained by the disk diffusion method showed that their efficiency depends on the size and amount of NPs; the authors referred that the probable mechanisms consist of: 1) the damage caused to the cell membrane and the sulfide and phosphate groups of DNA and protein by the interaction with the NPs, and 2) the induction of Reactive oxygen species that can damage the cell membrane, DNA, and lead to cell death.

Balasubramanian et al. (2020), also evaluated the anticancer activity of the AuNPs produced and the results of cytotoxicity against HeLa cancer cells indicate that the inhibition capacity depends on the time and dose administered: the gold nanoparticles suppress the cell viability by 69.28 % with a dose of 200 μg / mL. In this same line, Vijayakumar (2019) prepared AuNPs with extracts of the fruits of *Aegle marmelos*, *Eugenia jambolana* and *Annona muricata*. The results indicate that the inhibition of cell viability depends on the concentration of the administered NPs, but it was also evidenced that the phytochemicals involved in stabilizing these also influence their cytotoxicity, the NPs reduced with Annona were 30% more effective than the others with concentrations of 120 μg / mL.

Iron

Iron nanoparticles, FexOy and FeOOH (a total of 16 polymorphic structures) attract increasing interest due to the rapid development of their applications (Kharissova et al., 2013), among these Katata-Seru and collaborators (2018) evaluated the antibacterial effectiveness of FeNPs obtained by green reduction with *Moringa oleifera* leaves and seeds (MOL-FeNPS and MOS-FeNPs) against antibiotics such as ampicillin, gentamicin, erythromycin and vancomycin on gram negative strains; the results show that MOS-FeNPs are more effective than MOL-FeNPs against *E. coli* because they are the smallest NPs. The authors considered that the positive charge of the Fe ions may be responsible for the antibacterial activity through the attraction between the negative charge of the cell membrane of microorganisms.

Huang et al. (2014), obtained FeNPs by bioreduction using green tea, black tea and oolong tea (GT-FeNPs, BT-FeNPs and OT-FeNPS respectively) to apply them in a comparative study aiming to remove malachite green dye (GM); the results indicate that the highest efficiency was obtained with GT-FeNPs (81.6%). The authors suggested that the polyphenol molecules associated with the NPs of Fe which, by inducing its corrosion, allows the release of electrons capable of breaking the –C = C- and –C = N- bonds in the benzene rings. On the other hand, Devatha and collaborators (2016) evaluated the FeNPs obtained by green reduction of with *Mangifera indica* extracts (MI-FeNPs), *Murraya koenigii* (MK-FeNPs), *Azadirachta indica* (AI-FeNPs) and *Magnolia champaca* (MC-FeNPs).

For the treatment of domestic wastewater, the results indicate that the best treatment is obtained with AI -FeNPs with a removal efficiency of 98.1%, 84.3% and 82.4% for phosphates, ammoniacal nitrogen and COD respectively, using 1 g / L of NPs. Ouyang et al. (2019), carried out the reduction of Fe with a pure extract of polyphenols, to evaluate its catalytic capacity in the removal of Lincomycin (LCM), for which various systems were tested with NPs (GFe0.25, GFe0.5 and GFe1.0), it was found that with the GFe0.5 the degradation rate of the MCL after 90 min was 93.85% using a dose of 0.01 g / L.

Copper

Copper oxide (CuO) is an important semiconductor metal oxide with a band gap of 1.7 eV that can be obtained by green reduction and be used in the formulation of pesticides, fungicides and antibacterials, such as Ghidan et al. (2016) who evaluated CuO nanoparticles obtained by bioreduction with *Punica granatum* to eliminate the green peach aphid with an 86% efficiency in percentage of mortality, using a 8000 μg / mL concentration of NPs. Ilger et al. (2021), on the other hand, evaluated the effect of Cu NPs obtained with *Eucalyptus globulus* L. against the fungus *Colletotrichum capsici*, which causes rotting of chili fruit that affects farmers in India, the results obtained showed that concentrations of 500 ppm and 1000 ppm of NPs inhibit micellar growth completely. In addition they prolong the incubation period by reducing the number and length of the lesions caused by this fungus. Gopalakrishnan and Muniraj (2019) obtained CuNPs with *Azadirachta indica*, tested its antibacterial activity against *Enterococcus faecalis*, *Proteus mirabilis*, *Klebsiella pneumonia* and *Staphylococcus aureus* and obtained a high efficiency against *P. mirabilis* using 40 μg / mL of NPs.

In the medical area CuONPs have been evaluated as anti-inflammatory and anti-nociceptive in mice as reported by Liu et al. (2020), who obtained CuONPs by bioreduction with *Abies spectabilis*, their results indicate that CuONPs are effective by inhibiting noniceptive and inflammatory responses in mice with administered doses of 15 μg / Kg without producing behavioral changes in them, however, more studies are required to understand the exact therapeutic mechanisms. CuNPs have also been evaluated for wastewater treatment: Khani et al. (2018), reduced copper using *Ziziphus spina-christi* (L.) Willd. To apply the NPs obtained in the adsorption of the crystal violet dye, after optimizing the process, it was found that with the conditions of pH 9.0, dye concentration of 35 μg / mL, stirring time 7.5 min and 80 mg amount of sorbent, the removal efficiency reached 95%.

Zinc

Zinc oxide (ZnO) exists within the earth's crust as a mineral, zincite, however, most of it that is used commercially is obtained from synthetic methods. ZnO is not toxic and is compatible with human skin, making it an acceptable additive for textiles and surfaces that are in direct contact with the skin (Mirzaei & Darroudi, 2017). ZnO NPs have been tested as antimicrobial, Gunalan et al. (2012), performed the bioreduction of ZnO with aloe extract to evaluate its antimicrobial activity compared with NPs prepared by a chemical method, the results obtained for the minimum inhibitory concentration (MIC) suggest that the small NPs prepared by the green method show an improved microbicidal activity due to the greater surface area in relation to volume. The authors observed that ZnO NPs have a selective antimicrobial activity for both the bacteria and fungi evaluated; therefore, they considered that these constitute an effective agent against pathogenic microorganisms. Later, Santhoshkumar et al. (2017) obtained ZnO from green reduction with *Passiflora caerulea* to evaluate its antimicrobial activity against urinary tract pathogens such as *E. coli*, *Streptococcus sp*., *Enterococcus sp*., *Klebsiella sp*. The results showed that NPs have a dose-dependent effect, having a greater effectiveness for gram- than for gram + bacteria.The authors pointed out that NPs have different mechanisms of action against bacteria due to their structural differences.

In the medical area, Tettey and Shin (2019) synthesized ZnO NPs with *Scutellaria baicalensis* root extract, to evaluate its antioxidant and cytotoxic activity, in terms of antioxidant activity it was observed that it is dependent on the applied dose, namely it increases with increasing dose, in comparison with a standard antioxidant, the effectiveness was low, which the authors explained was not conclusive, thus they recommended more explorations in this regard. Regarding the cytotoxic activity, it was observed that the antiproliferative activity is also dose-dependent when tested against the growth of HeLa cells, the main possible mechanism according to the authors is the generation of free radicals that induce apoptosis in these cells, though they were tested with cells of the immune system and did not show toxicity at concentrations up to 1 mg / mL, which suggests that these NPs generated by green pathways could be promising candidates for the design of agents with a combined antioxidant and anticancer effect.

7.2 Bimetallic particles

Bimetallic nanoparticles differ from monometallic ones in that they contain two metallic ingredients, for their preparation from two precursor salts, two methods can be adopted:

1) co-reduction, which is the simultaneous reduction of two metals and 2) successive reduction in the that one metal is reduced over the nuclei of the other. Depending on the method used, nanoparticles will be produced in alloy or in layers (core-shell). Alloys have received increased attention due to the possibility of setting their properties over a wide range, simply by varying the composition of the alloy (Sumbal et al., 2019; Thakore et al., 2019). Bimetallic nanoparticles are of great interest for their applications in catalysis, electronics, as optical materials and coatings, and various methods have been reported to obtain them, however, reports on green routes to obtain bimetallic NPs are still few (Lagashetty et al., 2019; Schabes-Retchkiman et al., 2006).

Regarding the applications in the medical area, bimetallic NPs have been tested in antibacterial studies such as the one carried out by Al-Haddad et al. (2019), where they implemented the green reduction of bimetallic Cu-Ag particles with extract of *Phoenix dactylifera* leaves, evaluating the antibacterial activity of NPs against gram-positive and gram-negative results indicate that the bimetallic system exhibited good bacterial resistance at very low concentrations with an inhibition zone greater than 20 mm for both strains. Lagashetty et al. (2019), obtained Ag-Au bimetallic NPs by green reduction with Piper betle against *Bacillus subtils* and *Klebsiella planticola* strains: the results indicate that NPs are more effective for *B. subtils*. Merugu et al. (2020), used *Borassus flabellifer* for the reduction of bimetallic NPs Ag / Cu and Cu / Zn, evaluating its antibacterial activity against *Alcaligenes faecalis, Staphylococcus aureus, Citrobacter freundii, Klebsiella pneumonia* and *Clostridium perfringens,* the results indicate that NPs Ag / Cu and Cu / Zn are more effective than the tested control drugs (ciprofloxacin and amoxicillin), except for *Staphylococcus aureus* where amoxicillin showed better results.

In studies on anticancer and antioxidant activity, Elemike et al. (2019), developed a Ag-Au bimetallic system using *Stigmaphyllon ovatum* to test its cytotoxic capacity with HeLa cell lines; the results showed that, compared to bimetallic NPs the system showed greater activity due to possibly the synergistic effect of the two metals. According with the authors, the ability to inhibit cell viability is related to the ability of metals to generate Fenton-like reactions by means of which reactive oxygen species are produced that damage DNA and lead to cell death. In this same sense, Thakore et al. (2019), evaluated the cytotoxic effect of the Cu / Ag alloy bioreduced with sapota fruit latex, the tests with different proportions of the metals did not show cytotoxic effects, so its therapeutic application could lead to products biocompatible with the latex-coated alloy. Merugu et al. (2020), tested their bimetallic NPs against HeLa cancer cells and their antioxidant activity, with respect to the first test, the results indicate that the inhibition of cell viability increases with increasing dosage of NPs for both combinations Ag / Cu and Cu / Zn.

7.3 Biosynthesis of Fe / Cu bimetallic nanoparticles and their application in the removal of indigo carmine

One other area to use of NPs is in environmental remediation, specifically the treatment of water and wastewater through Advanced Oxidation Processes (AOP); this is a group of techniques that consider the environment the subject for the elimination of persistent organic pollutants, pathogens and by-products of water disinfection through the *in situ* formation of powerful oxidizing agents such as the hydroxyl radical ($HO^{\bullet}$). One of these processes is the Fenton reaction, which is based on the decomposition of hydrogen peroxide catalyzed by iron ions in an acid medium, among its main advantages are its low cost, ease of application at room temperature and ambient pressure. However, one of its main disadvantages lies in the high amounts of iron necessary to carry out the process (50-80 mg / mL) (Oruç et al. 2019; Scaria et al. 2020). Recently, the use of bimetallic catalysts (Elias E. Elemike et al. 2019; Xiulan Weng et al. 2017; Zhu et al. 2018) has shown that they have a better catalytic activity as result of the surface area increase and the synergistic effect between the two metals, which not only improves the degradation of pollutants complexes, but it is also useful to achieve the complete mineralization of their by-products. In this sense the Fe-Cu bimetallic catalysts have attracted attention because, as has been suggested, there is the interaction between the redox couple of the two Fe-Cu metals that could accelerate electronic transfer at the interface and thus improve the activation of H_2O_2 by the catalyst (Scaria et al. 2020; Sun et al. 2019; Tang & Wang, 2020; Wang et al. 2018).

Eucalyptus globulus belongs to the Myrtaceae family; due to its rapid growth which increases its timber biomass, the Eucalyptus genus is widely cultivated in the Mediterranean, its leaves are used for traditional remedies of several respiratory conditions (Boulekbache-Makhlouf et al. 2013).

Among its main components are holocellulose (83.2%), lignin (34.1%), and extractives (6.5%), where the latter are made up of lipophilic compounds and polyphenolic compounds responsible of its anti-inflammatory, antibacterial and antioxidant properties (González et al. 2017), the use of *Eucalyptus globulus* has already been reported for the synthesis of metallic nanoparticles (Iliger et al. 2021; Siripireddy & Mandal, 2017), its biomolecules play a key role in the reduction of ions at the nano scale and stabilization of nanoparticles (Iliger et al. 2021), in addition to being an economical and environmentally friendly method.

7.3.1 Materials and Methods

Preparation of the vegetal extract

Generally, the biosynthesis of metallic nanoparticles is carried out in aqueous solution (Amini et al. 2019), various authors agree on the procedure to obtain the plant extract, considering small variations such as plant organ used, amount of biomass per volume, boiling time (Agarwal et al. 2017; Ahmad et al. 2018; Rajesh et al. 2018; Siripireddy & Mandal, 2017).

In this research, eucalyptus leaves, moringa leaves and hibiscus flower were used to obtain the plant extract with which the Fe / Cu bimetallic particles were reduced. The leaves were acquired in the municipal market of Metepec, State of Mexico, transported to the laboratory and washed thoroughly to remove dirt and dust, then were placed in a paper bag in an oven at 100 °C for 24 hours, until they look completely dry. They were macerated to obtain a fine powder that was kept in an airtight container until use.

The infusions were prepared following the process reported by Siripireddy and Mandal (2017), namely: 10 g of eucalyptus, moringa and hibiscus leaf powder were weighed separately (Fig. 5.4); each sample was placed in a beaker and 70 mL distilled water were added, then the obtained suspensions were placed on a heating plate at constant stirring until boiling, the infusions were allowed to boil for 10-15 min, after which were removed and the supernatant was filtered, obtaining 50 mL of infusion. It was allowed to cool to room temperature and used for reduction reaction.

The three infusions prepared were tested to obtain Cu particles to evaluate which reducer was more efficient to be used to carry out the reduction reaction of the Fe / Cu bimetallic catalyst.

Figure 5.4 Procedure for the elaboration of the vegetal extract from eucalyptus leaves

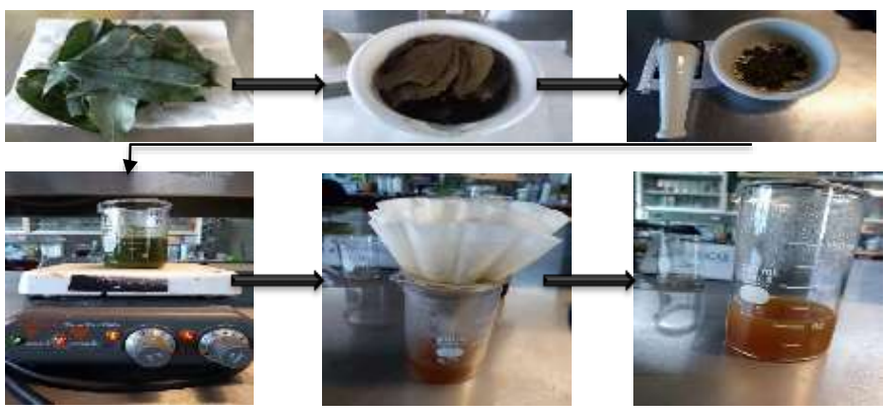

Own Elaboration

Reduction reaction

For the reduction reaction, 150 mL of $CuSO_4 \cdot 5H_2O$ 0.05 M were prepared with distilled water in a volumetric flask. The reduction reaction was carried out with the moringa extract plus the copper solution in a 1:1 volume ratio, at room temperature under constant stirring for one hour, but no color change was observed in the solution that remained a light green color, which suggested that the reduction process was not taking place (Fig. 5.5d). Subsequently, the hibiscus solution and the copper solution were tested under the same conditions; although the color change was not very evident, the resulting solution was filtered because a little turbidity was observed, obtaining very few particles (Fig. 5.5e).

Finally, the test with the eucalyptus infusion resulted in the color change from light brown of the infusion to dark brown that was due combination to reaction with the copper solution after the first 5 minutes (Fig. 5.5f), so this infusion was used as a reducing agent for the Fe / Cu bimetallic particles.

Figure 5.5. a), b) and c) infusions of moringa, hibiscus and eucalyptus before the reduction reaction; d), e) and f) solutions after one hour of reduction reaction with copper

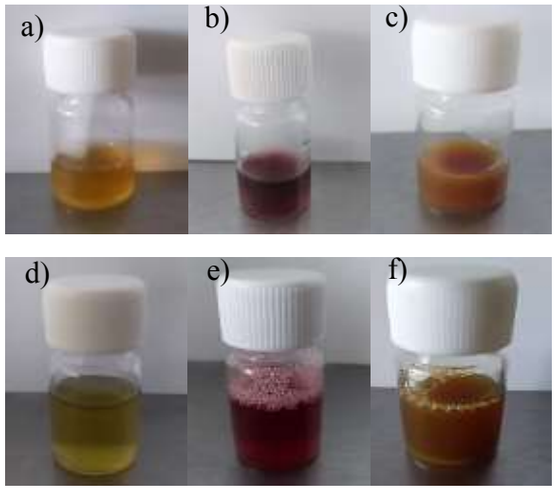

For the reduction of Fe / Cu bimetallic particles, 50 mL were prepared with $CuSO_4 \cdot 5H_2O$ and $FeSO_4 \cdot 7H_2O$ at a concentration of 0.05 M in distilled water, once the bimetallic solution had been prepared, the infusion of eucalyptus leaves (IEH) was added in a 1: 1 volume ratio, the color change from light brown to dark was observed immediately, the reaction was kept under constant stirring for 2 h, then the solution was left to rest for 24 h, after which it was filtered on a Büchner funnel; the particles obtained were dried at 70 °C for 48 hours and stored in 3 mL hermetic vials

Characterization of the Fe/Cu NPs

Determination of the SPR of the IEH-Sol containing Fe / Cu solution by means of UV-visible with a Perkin-Elmer Lambda 25 spectrophotometer.

Indigo carmine removal

Indigo carmine reagent grade was added with distilled water to set the pH with 4 M sulfuric acid and hydrogen peroxide at 30% analytical grade, the removal of the dye was monitored by UV-visible spectrophotometry with the Perkin-Elmer Lambda spectrophotometer 25, applying equation 4, the results obtained were fed into the statistical software Minitab Ver. 18.0 to design and carry out a factorial experimental 2^3; the factors evaluated were: dye concentration (200 - 400 mg / L), dose of 30% hydrogen peroxide (5 and 10 µL) and catalyst dose (1 and 5 mg). The volume used for each test was 10 mL at a pH of 3.0.

$$\% \text{ Remoción de IC} = \frac{C_0 - C_t}{C_0} * 100 \quad (4)$$

7.3.2 Results

Characterization of the Fe/Cu NPs

UV-vis spectrophotometry is a technique that allows establishing the formation of NPs (Katata-Seru et al. 2018), after the change in color of the infusion of eucalyptus leaves (IEH) from light brown to black after it enters into contact with the bimetallic solution; the reduction process is evidenced and the formation of nanoparticles due to surface plasmon resonance (SPR), as corroborated by the UV-vis absorption spectra that were obtained from the IEH, for the Fe / Cu bimetallic solution and for the reduction solution (IEH-Sol, Fe / Cu).

As seen in graph 1a) the IEH spectrum shows two absorption maxima at 270 and 220 nm, when added the bimetallic solution a decrease is observed in the maximum of 270 nm while that close to 200 nm increases reaching a maximum at 208 nm that corresponds to the bimetallic nanoparticles obtained. Graph 5.1b) shows the spectra corresponding to the individual reduction solutions of Fe / IEH and Cu / IEH; the spectrum of Fe / IEH agrees with that reported by Katata-Seru et al. (2018).

Graph 5.1 UV-Vis spectra: a) spectrum of the reduction reaction solutions in the green infusion of eucalyptus leaves plus iron and in the red infusion of eucalyptus leaves plus copper; b) spectra in the blue infusion of eucalyptus leaves (IEH), red bimetallic solution (Fe / Cu) and in green reduction solution (IEH-Sol. Fe / Cu)

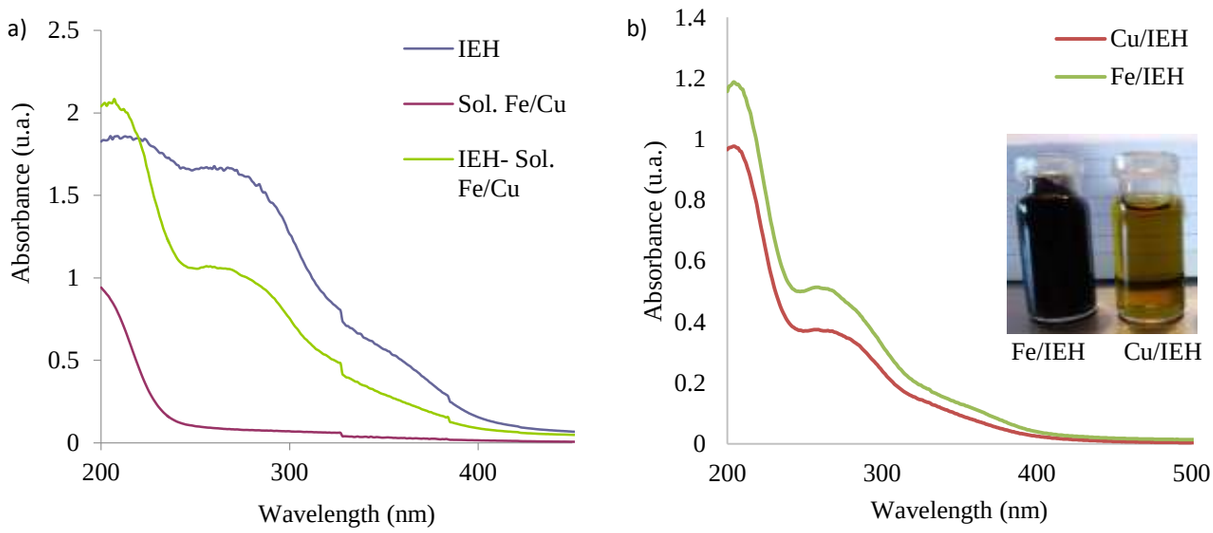

Proposed reduction mechanism

Eucalyptus (*Eucalyptus globulus*) is commonly used to treat respiratory diseases such as bronchitis, asthma, and influenza, among others; its antioxidant and antimicrobial capacity has been recognized by studies such as that of Boulekbache-Makhlouf et al. (2013), who found among its components the polyphenols, mainly hydrolysable tannins, responsible for said activity. Furthermore, Gonzales-Burgos et al. (2018), reported that among the flavonoids present in eucalyptus extracts the most abundant compound is chlorogenic acid and the group of quercetin glucosides which dispaly multiple hydroxyl groups that can act as reducing metal ions, as shown in the mechanism proposed in equation 5. Due to the redox potentials of the two metals (E^0 ($Fe_{(III)}$ / $Fe_{(II)}$) = 0.77 V) and Cu (E^0 ($Cu_{(II)}$ / $Cu_{(III)}$) = 0.17 V) it is proposed that iron reacts faster so that the Fe nuclei are the first to form to begin growth process, where the copper nanoparticles aggregate over the surface.

$$nCu^{2+} + nFe^{2+} + 4nAr\text{-}(OH)_n \rightarrow nFe(Cu)_{(s)} + 4n\ Ar{=}(O)_n + 4nH^+ \quad (5)$$

Indigo carmine removal

Preliminary calibration plots were made for the IC (Abs_{610} = 0.0447 (C_{IC}) - 0.0021) and the Isatin (Abs_{245} = 0.1655 (C_{Is}) - 0.0383), their main degradation by-product, obtaining a coefficient of determination of 0.9966 and 0.9981 respectively. Additionally, peroxide and Fe / Cu bimetallic particles were tested individually to observe their effect on color, as can be seen in graph 2, both peroxide and bimetallic particles remove color in very low percentage during the treatment time, 0.002 and 14.613% respectively.

Graph 5.2 Evaluation of the individual reagents for removal of the IC dye. Working conditions, volume: 10mL; dye concentration: 200 mg / L; pH: 3.0; amount of particles: 1mg; amount of H_2O_2: 10 µL

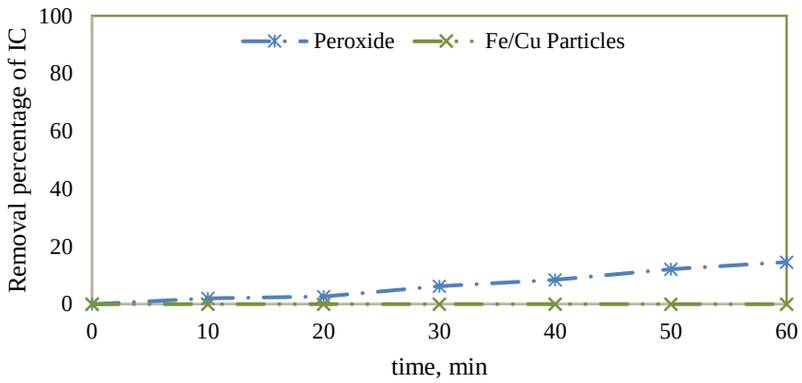

From the developed experimental design, a total of eight experiments were obtained with all possible combinations of the levels for each factor, each experiment was assigned the letters in alphabetical order A, B, C, D, E, F, G and H, all the experiments were carried out in triplicate, working with a set volume of 10 mL and with a set pH = 3.0.

Graph 5.3 Indigo carmine removal with Fenton-like reactions with Fe / Cu bimetallic nanoparticles: a) evaluation of the influence of the IC dye concentration (200 - 400 mg / L); b) evaluation of the influence of the amount of NPs Fe / Cu (1 - 5 mg); and c) evaluation of the influence of the H_2O_2 dose (5 - 10 µL). Working conditions: volume of 10 mL, pH 3.0, constant stirring (ANOVA analysis $p < 0.05$)

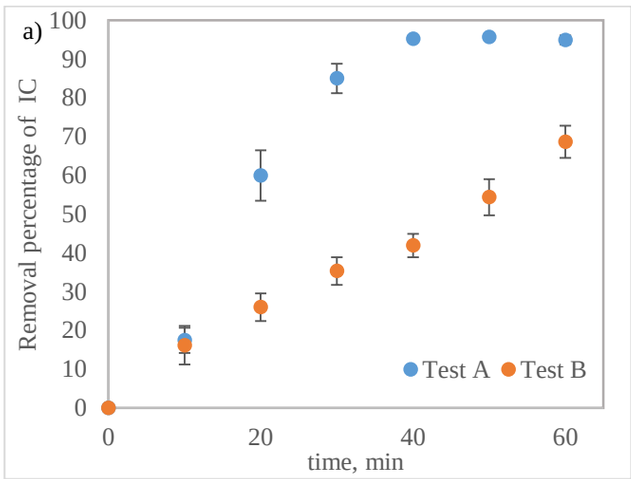

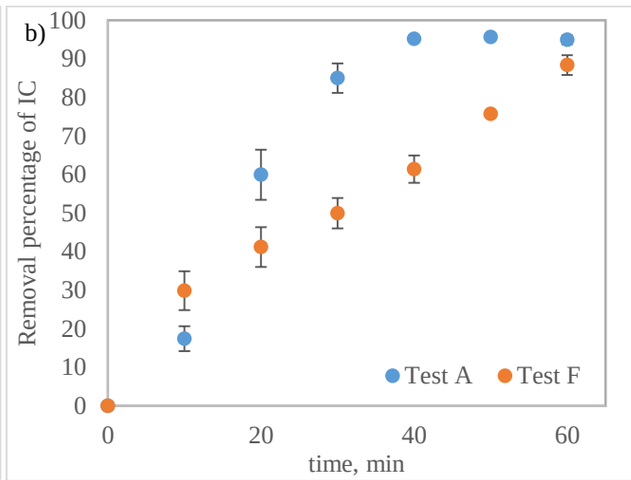

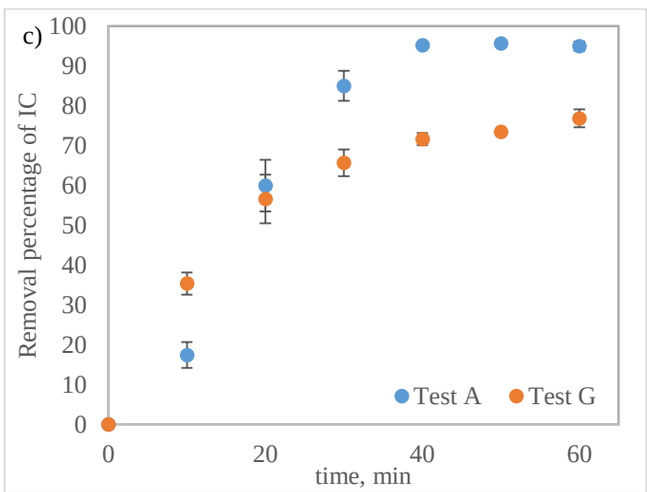

Regarding the effect of the concentration of the dye, as can be seen in graph 5.3a), when the dose of H_2O_2 (10 µL) and Fe / Cu bimetallic particles (5 mg) are kept constant, increasing the concentration of dye from 200 mg / L (test A) to 400 mg / L (test B).

The removal percentage is significantly decreased (ANOVA $p < 0.05$) from 94.92 to 68.66%, it is also important to note that after 40 minutes of test A maximum removal was reached. When analyzing the effect of the catalyst dose in graph 3b), it is apparent that by reducing the amount of catalyst (from 5 to 1 mg), keeping the dye concentration (200 mg) and the H_2O_2 dose (10 µL) constant, the removal percentage decreases from 94.92 to 88.37%, the effectiveness of the catalyst may be related to the standard reduction potentials of Fe (E^0 ($Fe_{(III)}$ / $Fe_{(II)}$) = 0.77 V) and Cu (E^0 ($Cu_{(II)}$ / $Cu_{(III)}$) = 0.17 V) where part of the Cu (I) generated on the Fe surface could promote Fe (II) regeneration through a thermodynamically favorable electron transfer process (6) (Tang & Wang, 2020).

$$Cu^{+} + Fe^{3+} \rightarrow Cu^{2+} + Fe^{2+} \qquad \Delta E^0 = 0.60\ V \tag{6}$$

The effect of H_2O_2 dosage (from 10 to 5 µL) can be observed in graph 3 c) also decreases the removal percentage from 94.92 to 76.83%; however, it is important to note that at 30 min in the G test, it exceeds 60% removal so that it is possible to reduce the H_2O_2 dose to an intermediate value and that this would not significantly affect the removal process and would also reduce the operating cost. It should be noted that since H_2O_2 is the main source of the $HO^{\bullet}$ radical, it is important that it is not insufficient since this generated a decrease in the degradation rate of the dye due to lower generation of $HO^{\bullet}$. Nonetheless, higher concentrations of H_2O_2 can be generated, more $HO^{\bullet}$ that may accelerate the decomposition of organic compounds, excess peroxide will have a predatory effect on $HO^{\bullet}$ radicals through the self-decomposition of H_2O_2 to O_2 and H_2O (equations 7-9) limiting the degradation process (Oruç et al. 2019).

$$H_2O_2 + HO^{\bullet} \rightarrow HO_2^{\bullet} + H_2O \tag{7}$$

$$HO_2^{\bullet} + HO^{\bullet} \rightarrow H_2O + O_2 \tag{8}$$

$$2H_2O_2 \rightarrow 2H_2O + O_2 \tag{9}$$

The analysis of variance (ANOVA) carried out in the statistical software Minitab Ver. 18.0, with a confidence level of 95%, using the IC percentage removal as the response variable in the analysis, shows that there are statistically significant differences ($p < 0.05$) between the different treatments, this suggests that the factors that have a greater effect on the response variable are the concentration of color and bimetallic particles. Since the value of R2 (94.31%) and fitted R2 (91.83%) are very close to 1.0, this indicates a good fit between the observations and that predicted by the model. The optimization of the experimental designates test A as the best.

UV-vis analysis of the Indigo Carmine removal

In the UV-vis spectra obtained from the indigo carmine dye (Fig. 5.6), two main absorption maxima can be identified as: the first in the visible region at 610 nm, typical of the IC dye, can be attributed to the orbital of the n → π group of the double bond system (transition of the non-binding electrons to the antiband π) and the second in the ultraviolet region at 287 nm characteristic of the benzene rings present in the molecule (aromatic compounds present absorption maxima between 210-320 nm).

Figure 5.6 Chemical structure of the indigo carmine *(modified from De León Condés et al., 2019)*

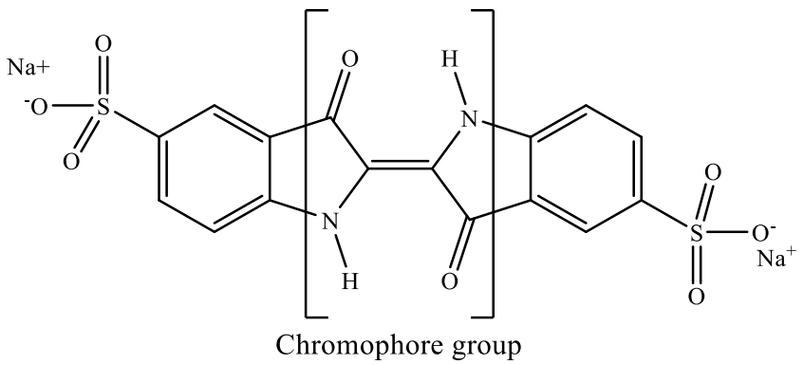

Graph 5.4 Indigo carmine UV-visible spectra: a) segment of the 200-400 nm range; b) segment of 550-700 nm characteristic absorption of the blue of the indigo carmine

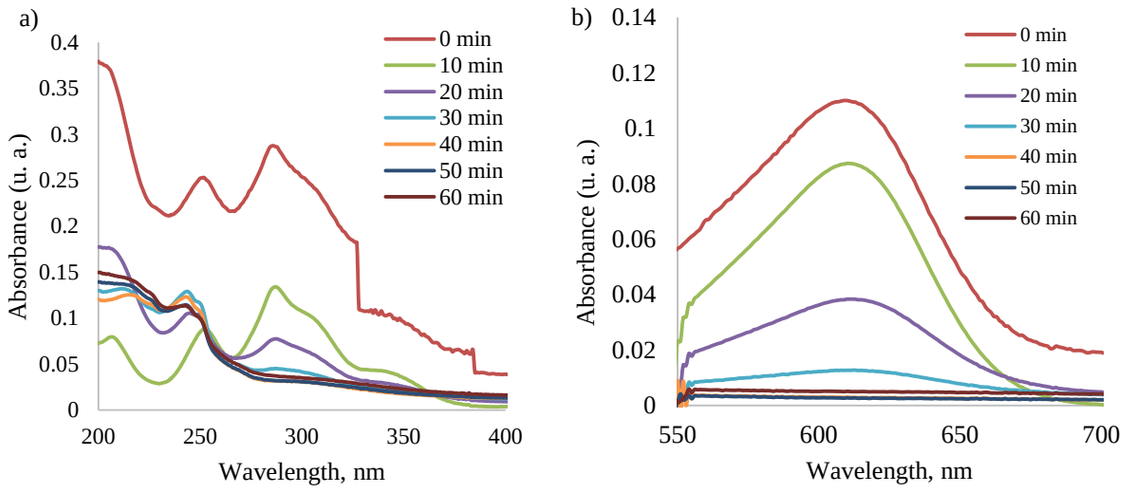

The graph 5.4b) shows the absorption band associated with the chromophore group of the dye molecule decreasing with time, which suggests an oxidation process by which the IC degrades during the first 30 minutes, while plot 4a) depicts the emergence of a maximum around 245 nm characteristic of isatin, that begins to be appear after 20 min reaction, reaching a maximum at 30 min; this decreases at the end of the experiment, therefore, in addition to the degradation of the IC , the main by-product generated from this process is also degraded, which is consistent with that reported by Torres-Blancas et al. (2017), who applied a Fe-Cu bimetallic catalyst in the ozonation process to remove the indigo carmine dye: this does not only improves the efficiency of the process, but also impacts the mineralization (90%) of its by-products in a short time through the generation of hydroxyl radicals. For the synergy of the ozonation, peroxidation, Fenton and Fenton-like concurrent reactions, much like the Fenton and Fenton-like processes evaluated with the Fe / Cu bimetallic particles, the reaction mechanism is very similar to that proposed by Torres-Blancas, shown in equation 10, where the generation of the $HO^{\bullet}$ radical can be seen responsible for the degradation of the indigo carmine dye.

$$Fe^{2+} + Cu^{2+} + 3H_2O_2 \rightarrow 3HO^{\bullet} + HO^{\bullet}_2 + H_2O + Fe^{3+} + Cu^{2+} \quad (10)$$

Bioreduction with eucalyptus is efficient to obtain monometallic and bimetallic Fe / Cu nanoparticles, which is verified through UV-Vis spectra of surface plasmon resonance (SPR) characteristic of nano-sized particles. The spectrum Fe / IEH is in close agreement with that reported in the literature at a wavelength of 208 nm. Thus, it is important to point out that the phytochemicals present in the eucalyptus extract are very important for the particles stability, to prevent their agglomeration, that would occur with other chemical reducers. The proposed mechanism suggests that iron ions are first reduced so that copper NPs deposit over their surface. The catalytic activity of the elaborated Fe / Cu bimetallic particles was tested for the removal of the indigo carmine dye in standard solutions through Fenton-like reactions, reaching an efficiency of 94.92% with optimal conditions, in addition to the removal of the Isatin by-product. Statistical analysis indicates that the concentration of the dye and the amount of bimetallic particles used have a significant effect on the removal of the dye.

8. Toxicity

The toxicity of nanomaterials depends on several factors such as: size, shape, size and shape of their distribution, surface charge and surface chemistry. To make a valid comparison in addition to the type of associated phytochemical, it is necessary to consider other factors such as reactivity, mobility, solubility and aggregation. (Amini, 2019; Sajid et al., 2015). Based on the review by Ajdary et al. (2018), NPs can enter the body through various means, like inhalation, skin and digestion; depending on their physicochemical characteristics and their method of preparation, NPs can access vital organs through blood flow and induce tissue and cell damage. Cell penetration occurs through diffusion intrusion, endocytosis, and membrane proteins such as the phospholipid layer; several investigations indicate that NPs activate oxidative stress by increasing the generation of reactive oxygen species (ROS), intervening in the expression of genes involved in inflammation, consequently generating damage to proteins, cell membrane and DNA (Fard et al., 2015).

Further, the presence of NPs in the environment gives rise to transformations capable of modifying their degree of toxicity, which still requires studies and test methods to single out the processes underway in different environmental spheres that allow identifying risk levels. (Zhang et al., 2018). Considering the above and the rapid growth, development, and applications of NPs, regulation via legislations, laws and rules are being implemented by various governmental organizations to minimize or avoid the risks associated with these materials. However, there are neither international regulations, nor protocols and legal terminology for management and production, nor toxicity tests or environmental impact assessments of NPs (Jeevanandam et al., 2018), so that management and production in research centers acquires relevant importance.

9. Conclusions

Bioreduction processes using plants show broad advantages over other methods related to the availability of plant species with antioxidant capacity, the complex matrix of the extract that provides not only chemical species with reducing capacities, but also provides stabilizing species that when associated with the surface of the NPs, can influence positively the application to be evaluated, mainly generating high expectations in the medical and catalytic area.

The manufacturing processes must consider the aforementioned aspects like pH, temperature, metal ion concentration, as well as the amount of plant extract, so it is important to carry out an optimization process to synthesize nanoparticles displaying the best qualities, which can be corroborated with the fundamental characterization studies such as UV-vis Spectrophotometry, X-ray Diffraction (XRD) and microscopy, either scanning electron microscopy (SEM) or transmission electron microscopy (TEM) to ensure the success of the tests to be carried out.

The application of bimetallic NPs obtained by bioreduction, as catalysts for advanced oxidation processes such as Fenton-like, is a viable field in development where high efficiencies can be found in the removal of organic pollutants; subsequent and complementary studies are required to shed light on the degree of mineralization of the pollutants and the toxicity of the particles used in the process.

Acknowledgements

The first author thanks CONACyT for the national scholarship granted for postgraduate studies, as well as the UAEMex 4986/2020 CIB Project for the finance provided; special thanks are given to the LIA María Citlali Martínez Soto for the support of the documentary film material, to the Dr. Mario Alberto Romero Romo for his support in the translation of this document.

References

Afsheen, S., Tahir, M. B., Iqbal, T., Liaqat, A., & Abrar, M. (2018). Green synthesis and characterization of novel iron particles by using different extracts. Journal of Alloys and Compounds, 732, 935–944. https://doi.org/10.1016/j.jallcom.2017.10.137

Agarwal, H., Kumar, S. V., & Rajeshkumar, S. (2017). A review on green synthesis of zinc oxide nanoparticles – An eco-friendly approach. Resource-Efficient Technologies, 3(4), 406–413. https://doi.org/10.1016/j.reffit.2017.03.002

Aghajanyan, A., Gabrielyan, L., Schubert, R., & Trchounian, A. (2020). Silver ion bioreduction in nanoparticles using Artemisia annua L. extract: characterization and application as antibacterial agents. AMB Express, 10. https://doi.org/10.1186/s13568-020-01002-w

Ahmad, T., Bustam, M. A., Irfan, M., Moniruzzaman, M., Anwaar Asghar, H. M., & Bhattacharjee, S. (2018). Green synthesis of stabilized spherical shaped gold nanoparticles using novel aqueous Elaeis guineensis (oil palm) leaves extract. Journal of Molecular Structure, 1159, 167–173. https://doi.org/10.1016/j.molstruc.2017.11.095

Ahmed, S., Saifullah, Ahmad, M., Swami, B. L., & Ikram, S. (2016). Green synthesis of silver nanoparticles using Azadirachta indica aqueous leaf extract. Journal of Radiation Research and Applied Sciences, 9, 1–7. https://doi.org/10.1016/j.jrras.2015.06.006

Ahmmad, B., Kurawaki, J., Ohkubo, T., & Kuroda, Y. (2013). GREEN TEA MEDIATED BIOSYNTHESIS OF -Fe 2 O 3 NANO - / MICRO-PARTICLES AND THEIR CHARACTERIZATION. World Journal of Engineering, December, 19–20.

Ajdary, M., Moosavi, M. A., Rahmati, M., Falahati, M., Mahboubi, M., Mandegary, A., Jangjoo, S., Mohammadinejad, R., & Varma, R. S. (2018). Health concerns of various nanoparticles: A review of their in vitro and in vivo toxicity. Nanomaterials, 8, 1–28. https://doi.org/10.3390/nano8090634

Al-Haddad, J., Alzaabi, F., Pal, P., Rambabu, K., & Banat, F. (2019). Green synthesis of bimetallic copper–silver nanoparticles and their application in catalytic and antibacterial activities. Clean Technologies and Environmental Policy, 22, 269–277. https://doi.org/10.1007/s10098-019-01765-2

Albeladi, S. S. R., Malik, M. A., & Al-Thabaiti, S. A. (2020). Facile biofabrication of silver nanoparticles using Salvia officinalis leaf extract and its catalytic activity towards Congo red dye degradation. Journal of Materials Research and Technology, 9, 10031–10044. https://doi.org/10.1016/j.jmrt.2020.06.074

Alwhibi, M. S., Soliman, D. A., al khaldy, H., Marraiki, N. A., El-Zaidy, M., & AlSubeie, M. S. (2020). Green biosynthesis of silver nanoparticle using Commiphora myrrh extract and evaluation of their antimicrobial activity and colon cancer cells viability. Journal of King Saud University - Science, 32, 3372–3379. https://doi.org/10.1016/j.jksus.2020.09.024

Amini, S. M. (2019). Preparation of antimicrobial metallic nanoparticles with bioactive compounds. Materials Science and Engineering C, 103(May), 109809. https://doi.org/10.1016/j.msec.2019.109809

Anu, K., Devanesan, S., Prasanth, R., AlSalhi, M. S., Ajithkumar, S., & Singaravelu, G. (2020). Biogenesis of selenium nanoparticles and their anti-leukemia activity. Journal of King Saud University - Science, 32(4), 2520–2526. https://doi.org/10.1016/j.jksus.2020.04.018

Araya-Castro, K., Chao, T. C., Durán-Vinet, B., Cisternas, C., Ciudad, G., & Rubilar, O. (2021). Green synthesis of copper oxide nanoparticles using protein fractions from an aqueous extract of brown algae macrocystis pyrifera. Processes, 9, 1–10. https://doi.org/10.3390/pr9010078

Arya, A., Gupta, K., & Chundawat, T. S. (2020). In vitro antimicrobial and antioxidant activity of biogenically synthesized palladium and platinum nanoparticles using botryococcus braunii. Turkish Journal of Pharmaceutical Sciences, 17, 299–306. https://doi.org/10.4274/tjps.galenos.2019.94103

Arya, A., Gupta, K., Chundawat, T. S., & Vaya, D. (2018). Biogenic Synthesis of Copper and Silver Nanoparticles Using Green Alga Botryococcus braunii and Its Antimicrobial Activity. Bioinorganic Chemistry and Applications, 2018. https://doi.org/10.1155/2018/7879403

Asghar, M. A., Zahir, E., Shahid, S. M., Khan, M. N., Asghar, M. A., Iqbal, J., & Walker, G. (2018). Iron, copper and silver nanoparticles: Green synthesis using green and black tea leaves extracts and evaluation of antibacterial, antifungal and aflatoxin B1 adsorption activity. LWT - Food Science and Technology, 90, 98–107. https://doi.org/10.1016/j.lwt.2017.12.009

Balasubramanian, S., Kala, S. M. J., & Pushparaj, T. L. (2020). Biogenic synthesis of gold nanoparticles using Jasminum auriculatum leaf extract and their catalytic, antimicrobial and anticancer activities. Journal of Drug Delivery Science and Technology, 57, 101620. https://doi.org/10.1016/j.jddst.2020.101620

Begum, J. P. S., Manjunath, K., Pratibha, S., Dhananjaya, N., Sahu, P., & Kashaw, S. (2020). Bioreduction synthesis of zinc oxide nanoparticles using Delonix regia leaf extract (Gul Mohar) and its agromedicinal applications. Journal of Science: Advanced Materials and Devices, 5, 468–475. https://doi.org/10.1016/j.jsamd.2020.07.009

Boulekbache-Makhlouf, L., Slimani, S., & Madani, K. (2013). Total phenolic content, antioxidant and antibacterial activities of fruits of Eucalyptus globulus cultivated in Algeria. Industrial Crops and Products, 41, 85–89. https://doi.org/10.1016/j.indcrop.2012.04.019

Canizal, G., Schabes-Retchkiman, P. S., Pal, U., Liu, H. B., & Ascencio, J. A. (2006). Controlled synthesis of Zn0 nanoparticles by bioreduction. Materials Chemistry and Physics, 97, 321–329. https://doi.org/10.1016/j.matchemphys.2005.08.015

Carrillo-Inungaray, M. L., Trejo-Ramirez, J. A., Reyes-Munguia, A., & Carranza-Alvarez, C. (2018). Advances and Perspectives. In Use of Nanoparticles in the Food Industry: Advances and Perspectives (Issue 6, pp. 419–444). Elsevier Inc. https://doi.org/10.1016/B978-0-12-811441-4/00015-7

Chamsa-ard, W., Fawcett, D., Fung, C. C., & Poinern, G. E. J. (2019). Biogenic synthesis of gold nanoparticles from waste watermelon and their antibacterial activity against Escherichia coli and Staphylococcus epidermidis. International Journal of Research in Medical Sciences, 7, 2499–2505. https://doi.org/10.18203/2320-6012.ijrms20192874

Chinnasamy, C., Tamilselvam, P., Karthick, B., Sidharth, B., & Senthilnathan, M. (2018). Green Synthesis, Characterization and Optimization Studies of Zinc Oxide Nano Particles Using Costusigneus Leaf Extract. Materials Today: Proceedings, 5(2), 6728–6735. https://doi.org/10.1016/j.matpr.2017.11.331

Cruz, D., Falé, P. L., Mourato, A., Vaz, P. D., Serralheiro, M. L., & Lino, A. R. L. (2010). Preparation and physicochemical characterization of Ag nanoparticles biosynthesized by Lippia citriodora (Lemon Verbena). Colloids and Surfaces B: Biointerfaces, 81(1), 67–73. https://doi.org/10.1016/j.colsurfb.2010.06.025

Dada, A. O., Adekola, F. A., Dada, F. E., Adelani-Akande, A. T., Bello, M. O., Okonkwo, C. R., Inyinbor, A. A., Oluyori, A. P., Olayanju, A., Ajanaku, K. O., & Adetunji, C. O. (2019). Silver nanoparticle synthesis by Acalypha wilkesiana extract: phytochemical screening, characterization, influence of operational parameters, and preliminary antibacterial testing. Heliyon, 5(10), e02517. https://doi.org/10.1016/j.heliyon.2019.e02517

De León-Condés, C. A., Roa-Morales, G., Martínez-Barrera, G., Balderas-Hernández, P., Menchaca-Campos, C., & Ureña-Núñez, F. (2019). A novel sulfonated waste polystyrene / iron oxide nanoparticles composite: Green synthesis, characterization and applications. Journal of Environmental Chemical Engineering, 7, 102841. https://doi.org/10.1016/j.jece.2018.102841

Deeksha, B., Sadanand, V., Hariram, N., & Rajulu, A. V. (2021). Preparation and properties of cellulose nanocomposite fabrics with in situ generated silver nanoparticles by bioreduction method. Journal of Bioresources and Bioproducts, 6, 75–81. https://doi.org/10.1016/j.jobab.2021.01.003

Devatha, C. P., Thalla, A. K., & Katte, S. Y. (2016). Green synthesis of iron nanoparticles using different leaf extracts for treatment of domestic waste water. Journal of Cleaner Production, 139, 1425–1435. https://doi.org/10.1016/j.jclepro.2016.09.019

Dzimitrowicz, A., Jamroz, P., DiCenzo, G. C., Gil, W., Bojszczak, W., Motyka, A., Pogoda, D., & Pohl, P. (2018). Fermented juices as reducing and capping agents for the biosynthesis of size-defined spherical gold nanoparticles. Journal of Saudi Chemical Society, 22, 767–776. https://doi.org/10.1016/j.jscs.2017.12.008

Ealia, A. M., & Saravanakumar, M. P. (2017). A review on the classification, characterisation, synthesis of nanoparticles and their application. IOP Conference Series: Materials Science and Engineering, 263, 0–15. https://doi.org/10.1088/1757-899X/263/3/032019

Elemike, E. E., Onwudiwe, D. C., Nundkumar, N., Singh, M., & Iyekowa, O. (2019). Green synthesis of Ag, Au and Ag-Au bimetallic nanoparticles using Stigmaphyllon ovatum leaf extract and their in vitro anticancer potential. Materials Letters, 243, 148–152. https://doi.org/10.1016/j.matlet.2019.02.049

Elemike, Elias E., Onwudiwe, D. C., Fayemi, O. E., & Botha, T. L. (2019). Green synthesis and electrochemistry of Ag, Au, and Ag–Au bimetallic nanoparticles using golden rod (Solidago canadensis) leaf extract. Applied Physics A: Materials Science and Processing, 125(1), 0. https://doi.org/10.1007/s00339-018-2348-0

Fard, J. K., Jafari, S., & Eghbal, M. A. (2015). A review of molecular mechanisms involved in toxicity of nanoparticles. Advanced Pharmaceutical Bulletin, 5, 447–454. https://doi.org/10.15171/apb.2015.061
Fatimah, I., Hidayat, H., Nugroho, B. H., & Husein, S. (2020). Ultrasound-assisted biosynthesis of silver and gold nanoparticles using Clitoria ternatea flower. South African Journal of Chemical Engineering, 34, 97–106. https://doi.org/10.1016/j.sajce.2020.06.007

Forough, M., & Farhadi, K. (2010). Biological and green synthesis of silver nanoparticles. Turkish Journal of Engineering and Environmental Sciences, 34, 281–287. https://doi.org/10.3906/muh-1005-30
Gan, P. P., & Li, S. F. Y. (2012). Potential of plant as a biological factory to synthesize gold and silver nanoparticles and their applications. Reviews in Environmental Science and Bio/Technology, 11(2), 169–206. https://doi.org/10.1007/s11157-012-9278-7

Geetha, M. S., Nagabhushana, H., & Shivananjaiah, H. N. (2016). Green mediated synthesis and characterization of ZnO nanoparticles using Euphorbia Jatropa latex as reducing agent. Journal of Science: Advanced Materials and Devices, 1(3), 301–310. https://doi.org/10.1016/j.jsamd.2016.06.015

Ghareib, M., Abdallah, W., Tahon, M. A., & Tallima, A. (2019). Biosynthesis of Copper Oxide Nanoparticles Using the Preformed Biomass of Aspergillus Fumigatus and Their. Digest Journal of Nanomaterials and Biostructures, 14, 291–303.

Ghidan, A. Y., Al-Antary, T. M., & Awwad, A. M. (2016). Green synthesis of copper oxide nanoparticles using Punica granatum peels extract: Effect on green peach Aphid. Environmental Nanotechnology, Monitoring and Management, 6, 95–98. https://doi.org/10.1016/j.enmm.2016.08.002

Ghosh, S., Patil, S., Ahire, M., Kitture, R., Gurav, D. D., Jabgunde, A. M., Kale, S., Pardesi, K., Shinde, V., Bellare, J., Dhavale, D. D., & Chopade, B. A. (2012). Gnidia glauca flower extract mediated synthesis of gold nanoparticles and evaluation of its chemocatalytic potential. Journal of Nanobiotechnology, 10, 1–9. https://doi.org/10.1186/1477-3155-10-17

González-Burgos, E., Liaudanskas, M., Viškelis, J., Žvikas, V., Janulis, V., & Gómez-Serranillos, M. P. (2018). Antioxidant activity, neuroprotective properties and bioactive constituents analysis of varying polarity extracts from Eucalyptus globulus leaves. Journal of Food and Drug Analysis, 26, 1293–1302. https://doi.org/10.1016/j.jfda.2018.05.010

González, N., Elissetche, J., Pereira, M., & Fernández, K. (2017). Extraction of polyphenols from Eucalyptus nitens and Eucalyptus globulus: Experimental kinetics, modeling and evaluation of their antioxidant and antifungical activities. Industrial Crops and Products, 109, 737–745. https://doi.org/10.1016/j.indcrop.2017.09.038

Gopalakrishnan, V., & Muniraj, S. (2019). Neem flower extract assisted green synthesis of copper nanoparticles - Optimisation, characterisation and anti-bacterial study. Materials Today: Proceedings, 36, 832–836. https://doi.org/10.1016/j.matpr.2020.07.013

Gunalan, S., Sivaraj, R., & Rajendran, V. (2012). Green synthesized ZnO nanoparticles against bacterial and fungal pathogens. Progress in Natural Science: Materials International, 22(6), 693–700. https://doi.org/10.1016/j.pnsc.2012.11.015

He, S., Guo, Z., Zhang, Y., Zhang, S., Wang, J., & Gu, N. (2007). Biosynthesis of gold nanoparticles using the bacteria Rhodopseudomonas capsulata. Materials Letters, 61, 3984–3987. https://doi.org/10.1016/j.matlet.2007.01.018

Hitesh, & Lata, S. (2018). Green Chemistry Based Synthesis of Silver Nanoparticles from Floral Extract of Nelumbo Nucifera. Materials Today: Proceedings, 5, 6227–6233. https://doi.org/10.1016/j.matpr.2017.12.231

Huang, L., Weng, X., Chen, Z., Megharaj, M., & Naidu, R. (2014). Green synthesis of iron nanoparticles by various tea extracts: Comparative study of the reactivity. Spectrochimica Acta - Part A: Molecular and Biomolecular Spectroscopy, 130, 295–301. https://doi.org/10.1016/j.saa.2014.04.037

Iliger, K. S., Sofi, T. A., Bhat, N. A., Ahanger, F. A., Sekhar, J. C., Elhendi, A. Z., Al-Huqail, A. A., & Khan, F. (2021). Copper nanoparticles: Green synthesis and managing fruit rot disease of chilli caused by Colletotrichum capsici. Saudi Journal of Biological Sciences, 28, 1477–1486. https://doi.org/10.1016/j.sjbs.2020.12.003

Jamdagni, P., Khatri, P., & Rana, J. S. (2018). Green synthesis of zinc oxide nanoparticles using flower extract of Nyctanthes arbor-tristis and their antifungal activity. Journal of King Saud University - Science, 30(2), 168–175. https://doi.org/10.1016/j.jksus.2016.10.002

Jamkhande, P. G., Ghule, N. W., Bamer, A. H., & Kalaskar, M. G. (2019). Metal nanoparticles synthesis: An overview on methods of preparation, advantages and disadvantages, and applications. Journal of Drug Delivery Science and Technology, 53, 101174. https://doi.org/10.1016/j.jddst.2019.101174

Jeevanandam, J., Barhoum, A., Chan, Y. S., Dufresne, A., & Danquah, M. K. (2018). Review on nanoparticles and nanostructured materials: History, sources, toxicity and regulations. Beilstein Journal of Nanotechnology, 9, 1050–1074. https://doi.org/10.3762/bjnano.9.98

Joshi, N., Filip, J., Coker, V. S., Sadhukhan, J., Safarik, I., Bagshaw, H., & Lloyd, J. R. (2018). Microbial reduction of Natural Fe(III) minerals; Toward the sustainable production of functional magnetic nanoparticles. Frontiers in Environmental Science, 6, 1–11. https://doi.org/10.3389/fenvs.2018.00127

Kalpana, V. N., Kataru, B. A. S., Sravani, N., Vigneshwari, T., Panneerselvam, A., & Devi Rajeswari, V. (2018). Biosynthesis of zinc oxide nanoparticles using culture filtrates of Aspergillus niger: Antimicrobial textiles and dye degradation studies. OpenNano, 3, 48–55. https://doi.org/10.1016/j.onano.2018.06.001

Katata-Seru, L., Moremedi, T., Aremu, O. S., & Bahadur, I. (2018). Green synthesis of iron nanoparticles using Moringa oleifera extracts and their applications: Removal of nitrate from water and antibacterial activity against Escherichia coli. Journal of Molecular Liquids, 256, 296–304. https://doi.org/10.1016/j.molliq.2017.11.093

Khani, R., Roostaei, B., Bagherzade, G., & Moudi, M. (2018). Green synthesis of copper nanoparticles by fruit extract of Ziziphus spina-christi (L.) Willd.: Application for adsorption of triphenylmethane dye and antibacterial assay. Journal of Molecular Liquids, 255, 541–549. https://doi.org/10.1016/j.molliq.2018.02.010

Khanna, P., Kaur, A., & Goyal, D. (2019). Algae-based metallic nanoparticles: Synthesis, characterization and applications. Journal of Microbiological Methods, 163, 105656. https://doi.org/10.1016/j.mimet.2019.105656

Kharissova, O. V., Rasika, H. V., Kharisov, B. I., Olvera, B., & Jiménez, V. M. (2013). The greener synthesis of nanoparticles. Trends in Biotechnology, 31(4), 240–248. https://doi.org/10.1016/j.tibtech.2013.01.003

Korkmaz, N. (2020). Bioreduction: The biological activity, characterization, and synthesis of silver nanoparticles. Turkish Journal of Chemistry, 44, 325–334. https://doi.org/10.3906/KIM-1910-8

Kuppusamy, P., Yusoff, M. M., Maniam, G. P., & Govindan, N. (2016). Biosynthesis of metallic nanoparticles using plant derivatives and their new avenues in pharmacological applications – An updated report. Saudi Pharmaceutical Journal, 24(4), 473–484. https://doi.org/10.1016/j.jsps.2014.11.013

Lagashetty, A., Ganiger, S. K., & Shashidhar. (2019). Synthesis, characterization and antibacterial study of Ag–Au Bi-metallic nanocomposite by bioreduction using piper betle leaf extract. Heliyon, 5, e02794. https://doi.org/10.1016/j.heliyon.2019.e02794

Li, J., Li, Q., Ma, X., Tian, B., Li, T., Yu, J., Dai, S., Weng, Y., & Hua, Y. (2016). Biosynthesis of gold nanoparticles by the extreme bacterium Deinococcus radiodurans and an evaluation of their antibacterial properties. International Journal of Nanomedicine, 11, 5931–5944. https://doi.org/10.2147/IJN.S119618

Liu, H., Zheng, S. M., Xiong, H. F., Alwahibi, M. S., & Niu, X. (2020). Biosynthesis of copperoxide nanoparticles using Abies spectabilis plant extract and analyzing its antinociceptive and anti-inflammatory potency in various mice models. Arabian Journal of Chemistry, 13, 6995–7006. https://doi.org/10.1016/j.arabjc.2020.07.006

Makarov, V. V., Love, A. J., Sinitsyna, O. V., Makarova, S. S., Yaminsky, I. V., Taliansky, M. E., & Kalinina, N. O. (2014). "Green" nanotechnologies: Synthesis of metal nanoparticles using plants. Acta Naturae, 6(20), 35–44. https://doi.org/10.32607/20758251-2014-6-1-35-44

Mallikarjuna, K., Narasimha, G., Dillip, G. R., Praveen, B., Shreedhar, B., Lakshmi, C. S., Reddy, B. V. S., & Raju, B. D. P. (2011). Green synthesis of silver nanoparticles using Ocimum leaf extract and their characterization. Digest Journal of Nanomaterials and Biostructures, 6, 181–186.

Matinise, N., Fuku, X. G., Kaviyarasu, K., Mayedwa, N., & Maaza, M. (2017). ZnO nanoparticles via Moringa oleifera green synthesis: Physical properties & mechanism of formation. Applied Surface Science, 406, 339–347. https://doi.org/10.1016/j.apsusc.2017.01.219

Merugu, R., Gothalwal, R., Deshpande, P. K., De Mandal, S., Padala, G., & Chitturi, K. L. (2020). Synthesis of Ag/Cu and Cu/Zn bimetallic nanoparticles using toddy palm: Investigations of their antitumor, antioxidant and antibacterial activities. Materials Today: Proceedings. https://doi.org/10.1016/j.matpr.2020.08.027

Mirzaei, H., & Darroudi, M. (2017). Zinc oxide nanoparticles: Biological synthesis and biomedical applications. Ceramics International, 43, 907–914. https://doi.org/10.1016/j.ceramint.2016.10.051

Mishra, B., Saxena, A., & Tiwari, A. (2020). Biosynthesis of silver nanoparticles from marine diatoms Chaetoceros sp., Skeletonema sp., Thalassiosira sp., and their antibacterial study. Biotechnology Reports, 28, e00571. https://doi.org/10.1016/j.btre.2020.e00571

Mohaghegh, S., Osouli-Bostanabad, K., Nazemiyeh, H., Javadzadeh, Y., Parvizpur, A., Barzegar-Jalali, M., & Adibkia, K. (2020). A comparative study of eco-friendly silver nanoparticles synthesis using Prunus domestica plum extract and sodium citrate as reducing agents. Advanced Powder Technology, 31, 1169–1180. https://doi.org/10.1016/j.apt.2019.12.039

Mukunthan, K. S., Elumalai, E. K., Patel, T. N., & Murty, V. R. (2011). Catharanthus roseus: A natural source for the synthesis of silver nanoparticles. Asian Pacific Journal of Tropical Biomedicine, 1, 270–274. https://doi.org/10.1016/S2221-1691(11)60041-5

Nagar, N., & Devra, V. (2018). Green synthesis and characterization of copper nanoparticles using Azadirachta indica leaves. Materials Chemistry and Physics, 213, 44–51. https://doi.org/10.1016/j.matchemphys.2018.04.007

Narayanan, K. B., & Sakthivel, N. (2010a). Phytosynthesis of gold nanoparticles using leaf extract of Coleus amboinicus Lour. Materials Characterization, 61, 1232–1238. https://doi.org/10.1016/j.matchar.2010.08.003

Narayanan, K. B., & Sakthivel, N. (2010b). Biological synthesis of metal nanoparticles by microbes. Advances in Colloid and Interface Science, 156, 1–13. https://doi.org/10.1016/j.cis.2010.02.001

Nasrollahzadeh, M., Sajjadi, M., Dadashi, J., & Ghafuri, H. (2020). Pd-based nanoparticles: Plant-assisted biosynthesis, characterization, mechanism, stability, catalytic and antimicrobial activities. Advances in Colloid and Interface Science, 276, 102103. https://doi.org/10.1016/j.cis.2020.102103

Nava, O. J., Soto-Robles, C. A., Gómez-Gutiérrez, C. M., Vilchis-Nestor, A. R., Castro-Beltrán, A., Olivas, A., & Luque, P. A. (2017). Fruit peel extract mediated green synthesis of zinc oxide nanoparticles. Journal of Molecular Structure, 1147, 1–6. https://doi.org/10.1016/j.molstruc.2017.06.078

Nayantara, & Kaur, P. (2018). Biosynthesis of nanoparticles using eco-friendly factories and their role in plant pathogenicity: a review. Biotechnology Research and Innovation, 2, 63–73. https://doi.org/10.1016/j.biori.2018.09.003

Ninganagouda, S., Rathod, V., Jyoti, H., Singh, D., Prema, K., & Manzoor-Ul-Haq. (2013). EXTRACELLULAR BIOSYNTHESIS OF SILVER NANOPARTICLES USING ASPERGILLUS FLAVUS AND THEIR ANTIMICROBIAL ACTIVITY AGAINST GRAM NEGATIVE MDR STRAINS. International Journal of Pharma and Bio Sciences, 4, 222–229.

Olajire, A. A., & Mohammed, A. A. (2020). Green synthesis of bimetallic PdcoreAushell nanoparticles for enhanced solid-phase photodegradation of low-density polyethylene film. Journal of Molecular Structure, 1206, 127724. https://doi.org/10.1016/j.molstruc.2020.127724

Oruç, Z., Ergüt, M., Uzunoğlu, D., & Özer, A. (2019). Green synthesis of biomass-derived activated carbon/Fe-Zn bimetallic nanoparticles from lemon (Citrus limon (L.) Burm. f.) wastes for heterogeneous Fenton-like decolorization of Reactive Red 2. Journal of Environmental Chemical Engineering, 7, 103231. https://doi.org/10.1016/j.jece.2019.103231

Ouyang, Q., Kou, F., Tsang, P. E., Lian, J., Xian, J., Fang, J., & Fang, Z. (2019). Green synthesis of Fe-based material using tea polyphenols and its application as a heterogeneous Fenton-like catalyst for the degradation of lincomycin. Journal of Cleaner Production, 232, 1492–1498. https://doi.org/10.1016/j.jclepro.2019.06.043

Ovais, M., Khalil, A. T., Ayaz, M., Ahmad, I., Nethi, S. K., & Mukherjee, S. (2018). Biosynthesis of metal nanoparticles via microbial enzymes: A mechanistic approach. International Journal of Molecular Sciences, 19, 1–20. https://doi.org/10.3390/ijms19124100

Powar, N. S., & Patel, V. (2019). Cu Nanoparticle : Synthesis , Characterization and Application Review article Cu Nanoparticle : Synthesis , Characterization and Application. Chemical Methodologies, 3(January), 457–480. https://doi.org/10.22034/chemm.2019.154075.1112

Rai, M., & Yadav, A. (2013). Plants as potential synthesiser of precious metal nanoparticles: Progress and prospects. IET Nanobiotechnology, 7, 117–124. https://doi.org/10.1049/iet-nbt.2012.0031

Rajesh, K. M., Ajitha, B., Reddy, Y. A. K., Suneetha, Y., & Reddy, P. S. (2018). Assisted green synthesis of copper nanoparticles using Syzygium aromaticum bud extract: Physical, optical and antimicrobial properties. Optik, 154, 593–600. https://doi.org/10.1016/j.ijleo.2017.10.074

Reddy, K. R. (2017). Green synthesis, morphological and optical studies of CuO nanoparticles. Journal of Molecular Structure, 1150, 553–557. https://doi.org/10.1016/j.molstruc.2017.09.005

Sajid, M., Ilyas, M., Basheer, C., Tariq, M., Daud, M., Baig, N., & Shehzad, F. (2015). Impact of nanoparticles on human and environment: review of toxicity factors, exposures, control strategies, and future prospects. Environmental Science and Pollution Research, 22(6), 4122–4143. https://doi.org/10.1007/s11356-014-3994-1

Salem, S. S., & Fouda, A. (2020). Green Synthesis of Metallic Nanoparticles and Their Prospective Biotechnological Applications: an Overview. Biological Trace Element Research, 199, 344–370. https://doi.org/10.1007/s12011-020-02138-3

Santhoshkumar, J., Kumar, S. V., & Rajeshkumar, S. (2017). Synthesis of zinc oxide nanoparticles using plant leaf extract against urinary tract infection pathogen. Resource-Efficient Technologies, 3, 459–465. https://doi.org/10.1016/j.reffit.2017.05.001

Saravanan, A., Kumar, P. S., Karishma, S., Vo, D. N., Jeevanantham, S., Yaashikaa, P. R., & George, C. S. (2021). A review on biosynthesis of metal nanoparticles and its environmental applications. Chemosphere, 264, 128580. https://doi.org/10.1016/j.chemosphere.2020.128580

Scaria, J., Nidheesh, P. V., & Kumar, M. S. (2020). Synthesis and applications of various bimetallic nanomaterials in water and wastewater treatment. Journal of Environmental Management, 259, 110011. https://doi.org/10.1016/j.jenvman.2019.110011

Schabes-Retchkiman, P. S., Canizal, G., Herrera-Becerra, R., Zorrilla, C., Liu, H. B., & Ascencio, J. A. (2006). Biosynthesis and characterization of Ti/Ni bimetallic nanoparticles. Optical Materials, 29, 95–99. https://doi.org/10.1016/j.optmat.2006.03.014

Selvan, D. A., Mahendiran, D., Kumar, R. S., & Rahiman, A. K. (2018). Garlic, green tea and turmeric extracts-mediated green synthesis of silver nanoparticles: Phytochemical, antioxidant and in vitro cytotoxicity studies. Journal of Photochemistry and Photobiology B: Biology, 180, 243–252. https://doi.org/10.1016/j.jphotobiol.2018.02.014

Shamsuzzaman, Mashrai, A., Khanam, H., & Aljawfi, R. N. (2017). Biological synthesis of ZnO nanoparticles using C. albicans and studying their catalytic performance in the synthesis of steroidal pyrazolines. Arabian Journal of Chemistry, 10, S1530–S1536. https://doi.org/10.1016/j.arabjc.2013.05.004

Sharma, A., Sharma, S., Sharma, K., Chetri, S. P. K., Vashishtha, A., Singh, P., Kumar, R., Rathi, B., & Agrawal, V. (2015). Algae as crucial organisms in advancing nanotechnology: a systematic review. Journal of Applied Phycology, 28, 1759–1774. https://doi.org/10.1007/s10811-015-0715-1

Sharma, D., Kanchi, S., & Bisetty, K. (2019). Biogenic synthesis of nanoparticles: A review. Arabian Journal of Chemistry, 12, 3576–3600. https://doi.org/10.1016/j.arabjc.2015.11.002

Sharmila, G., Pradeep, R. S., Sandiya, K., Santhiya, S., Muthukumaran, C., Jeyanthi, J., Kumar, N. M., & Thirumarimurugan, M. (2018). Biogenic synthesis of CuO nanoparticles using Bauhinia tomentosa leaves extract: Characterization and its antibacterial application. Journal of Molecular Structure, 1165, 288–292. https://doi.org/10.1016/j.molstruc.2018.04.011

Sherin, L., Sohail, A., Amjad, U., Mustafa, M., Jabeen, R., & Ul-Hamid, A. (2020). Facile green synthesis of silver nanoparticles using Terminalia bellerica kernel extract for catalytic reduction of anthropogenic water pollutants. Colloids and Interface Science Communications, 37, 100276. https://doi.org/10.1016/j.colcom.2020.100276

Silva-De Hoyos, L. E., Sánchez-Mendieta, V., Camacho-López, M. A., Trujillo-Reyes, J., & Vilchis-Nestor, A. R. (2020). Plasmonic and fluorescent sensors of metal ions in water based on biogenic gold nanoparticles. Arabian Journal of Chemistry, 13, 1975–1985. https://doi.org/10.1016/j.arabjc.2018.02.016

Silva-De Hoyos, L. E., Sánchez-Mendieta, V., Vilchis-Nestor, A. R., Camacho-López, M. A., Trujillo-Reyes, J., & Avalos-Borja, M. (2019). Plasmonic Sensing of Aqueous-Divalent Metal Ions by Biogenic Gold Nanoparticles. Journal of Nanomaterials, 2019, 1–12. https://doi.org/10.1155/2019/9846729

Singh, J., Dutta, T., Kim, K.-H., Rawat, M., Samddar, P., & Kumar, P. (2018). "Green" synthesis of metals and their oxide nanoparticles: applications for environmental remediation. Journal of Nanobiotechnology, 16, 1–24. https://doi.org/10.1186/s12951-018-0408-4

Siripireddy, B., & Mandal, B. K. (2017). Facile green synthesis of zinc oxide nanoparticles by Eucalyptus globulus and their photocatalytic and antioxidant activity. Advanced Powder Technology, 28, 785–797. https://doi.org/10.1016/j.apt.2016.11.026

Sumbal, Nadeem, A., Naz, S., Ali, J. S., Mannan, A., & Zia, M. (2019). Synthesis, characterization and biological activities of monometallic and bimetallic nanoparticles using Mirabilis jalapa leaf extract. Biotechnology Reports, 22, e00338. https://doi.org/10.1016/j.btre.2019.e00338

Sun, Y., Yang, Z., Tian, P., Sheng, Y., Xu, J., & Han, Y.-F. (2019). Oxidative degradation of nitrobenzene by a Fenton-like reaction with Fe-Cu bimetallic catalysts. Applied Catalysis B: Environmental, 244, 1–10. https://doi.org/10.1016/j.apcatb.2018.11.009

Tamuly, C., Hazarika, M., & Bordoloi, M. (2013). Biosynthesis of Au nanoparticles by Gymnocladus assamicus and its catalytic activity. Materials Letters, 108, 276–279. https://doi.org/10.1016/j.matlet.2013.07.020

Tang, J., & Wang, J. (2020). Iron-copper bimetallic metal-organic frameworks for efficient Fenton-like degradation of sulfamethoxazole under mild conditions. Chemosphere, 241, 125002. https://doi.org/10.1016/j.chemosphere.2019.125002

Tettey, C. O., & Shin, H. M. (2019). Evaluation of the antioxidant and cytotoxic activities of zinc oxide nanoparticles synthesized using scutellaria baicalensis root. Scientific African, 6, e00157. https://doi.org/10.1016/j.sciaf.2019.e00157

Thakore, S. I., Nagar, P. S., Jadeja, R. N., Thounaojam, M., Devkar, R. V., & Rathore, P. S. (2019). Sapota fruit latex mediated synthesis of Ag, Cu mono and bimetallic nanoparticles and their in vitro toxicity studies. Arabian Journal of Chemistry, 12, 694–700. https://doi.org/10.1016/j.arabjc.2014.12.042

Torres-Blancas, T., Roa-Morales, G., Ureña-Núñez, F., Barrera-Díaz, C., Dorazco-González, A., & Natividad, R. (2017). Ozonation enhancement by Fe–Cu biometallic particles. Journal of the Taiwan Institute of Chemical Engineers, 74, 225–232. https://doi.org/10.1016/j.jtice.2017.02.025

Umai, D., Vikranth, A., & Meenambiga, S. S. (2020). A study on the green synthesis of silver nanoparticles from Olea europaea and its activity against oral pathogens. Materials Today: Proceedings. https://doi.org/10.1016/j.matpr.2020.10.681

Vijayakumar, S. (2019). Eco-friendly synthesis of gold nanoparticles using fruit extracts and in vitro anticancer studies. Journal of Saudi Chemical Society, 23, 753–761. https://doi.org/10.1016/j.jscs.2018.12.002

Vijayakumar, S., Mahadevan, S., Arulmozhi, P., Sriram, S., & Praseetha, P. K. (2018). Green synthesis of zinc oxide nanoparticles using Atalantia monophylla leaf extracts: Characterization and antimicrobial analysis. Materials Science in Semiconductor Processing, 82, 39–45. https://doi.org/10.1016/j.mssp.2018.03.017

Vijayaraghavan, K., & Ashokkumar, T. (2017). Plant-mediated biosynthesis of metallic nanoparticles: A review of literature, factors affecting synthesis, characterization techniques and applications. Journal of Environmental Chemical Engineering, 5(5), 4866–4883. https://doi.org/10.1016/j.jece.2017.09.026

Wahab, A. W., Karim, A., Asmawati, & Sutapa, I. W. (2018). Bio-synthesis of gold nanoparticles through bioreduction using the aqueous extract of Muntingia calabura L. leaves. Oriental Journal of Chemistry, 34, 401–409. https://doi.org/10.13005/ojc/340143

Wang, Q., Ma, Y., & Xing, S. (2018). Comparative study of Cu-based bimetallic oxides for Fenton-like degradation of organic pollutants. Chemosphere, 203, 450–456. https://doi.org/10.1016/j.chemosphere.2018.04.013

Weng, X., Lin, Z., Xiao, X., Li, C., & Chen, Z. (2018). One-step biosynthesis of hybrid reduced graphene oxide/iron-based nanoparticles by eucalyptus extract and its removal of dye. Journal of Cleaner Production, 203, 22–29. https://doi.org/10.1016/j.jclepro.2018.08.158

Weng, Xiulan, Guo, M., Luo, F., & Chen, Z. (2017). One-step green synthesis of bimetallic Fe/Ni nanoparticles by eucalyptus leaf extract: Biomolecules identification, characterization and catalytic activity. Chemical Engineering Journal, 308, 904–911. https://doi.org/10.1016/j.cej.2016.09.134

Wu, J. W., & Ng, I. S. (2017). Biofabrication of gold nanoparticles by Shewanella species. Bioresources and Bioprocessing, 4. https://doi.org/10.1186/s40643-017-0181-5

Yasin, S., Liu, L., & Yao, J. (2013). Biosynthesis of silver nanoparticles by bamboo leaves extract and their antimicrobial activity. Journal of Fiber Bioengineering and Informatics, 6, 77–84. https://doi.org/10.3993/jfbi03201307

Yusof, H. M., Rahman, N. A., Mohamad, R., Zaidan, U. H., & Samsudin, A. A. (2020). Biosynthesis of zinc oxide nanoparticles by cell-biomass and supernatant of Lactobacillus plantarum TA4 and its antibacterial and biocompatibility properties. Scientific Reports, 10, 1–13. https://doi.org/10.1038/s41598-020-76402-w

Zayed, M. F., & Eisa, W. H. (2014). Phoenix dactylifera L. leaf extract phytosynthesized gold nanoparticles; Controlled synthesis and catalytic activity. Spectrochimica Acta - Part A: Molecular and Biomolecular Spectroscopy, 121, 238–244. https://doi.org/10.1016/j.saa.2013.10.092

Zhang, J., Guo, W., Li, Q., Wang, Z., & Liu, S. (2018). The effects and the potential mechanism of environmental transformation of metal nanoparticles on their toxicity in organisms. Environmental Science: Nano, 5, 2482–2499. https://doi.org/10.1039/c8en00688a

Zhu, F., Ma, S., Liu, T., & Deng, X. (2018). Green synthesis of nano zero-valent iron/Cu by green tea to remove hexavalent chromium from groundwater. Journal of Cleaner Production, 174, 184–190. https://doi.org/10.1016/j.jclepro.2017.10.302

Žvab, U., Kukulin, D. S., Fanetti, M., & Valant, M. (2021). Bioremediation of copper polluted wastewater-like nutrient media and simultaneous synthesis of stable copper nanoparticles by a viable green alga. Journal of Water Process Engineering, 42, 102123. https://doi.org/10.1016/j.jwpe.2021.102123